The Maersk Mc-Kinney Moller Institute

sdu.dk

#sdudk

Bridging Medical Robotics and Electrical Bio-Impedance

Cheng Zhuoqi

Email: zch@mmmi.sdu.dk

SDU

July 2021

Index

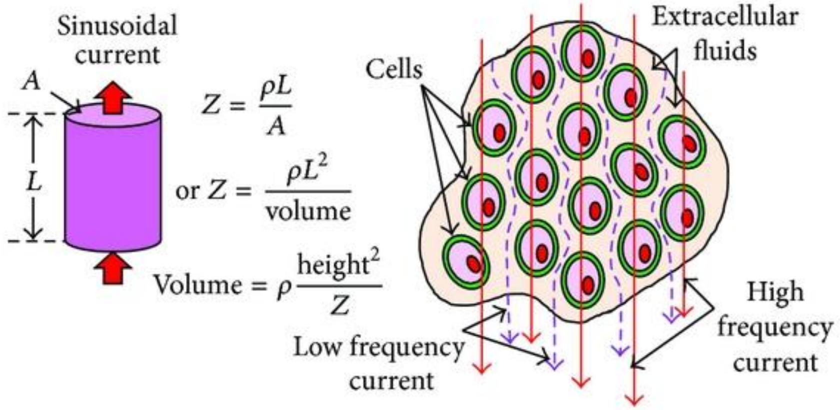

Electrical Bio-Impedance (EBI)

Sensing configurations

→ Monopolar
→ Bipolar
→ Tripolar
→ Tetrapolar

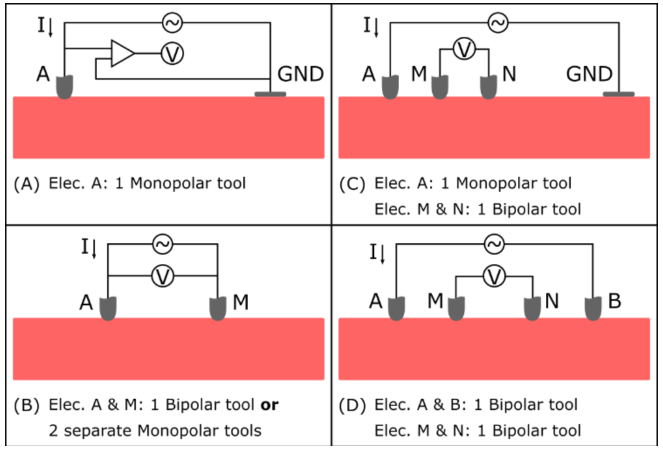

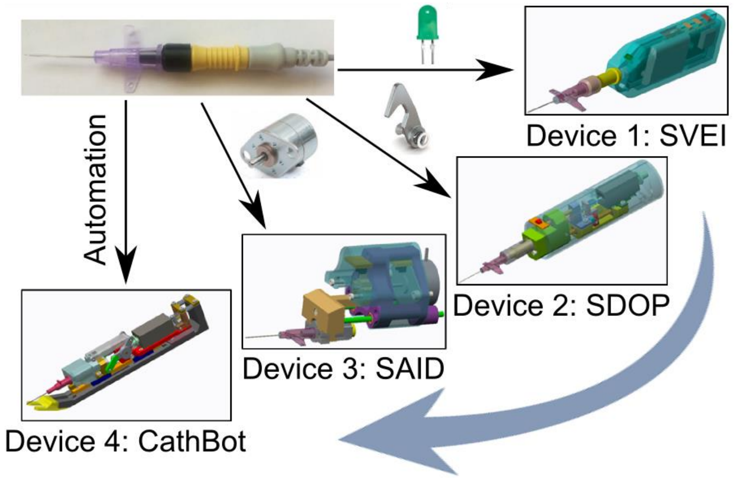

Handheld Robotic Device for Peripheral Intravenous Catheterization

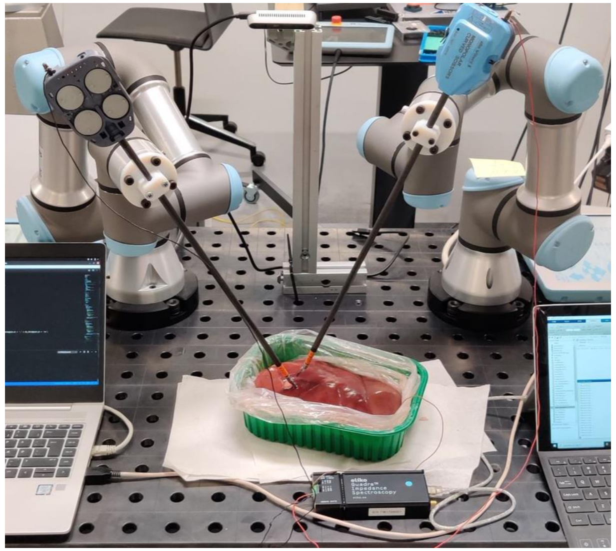

Robot Assisted Electrical Impedance Sensing (RAEIS)

Electrical Bio-Impedance (EBI)

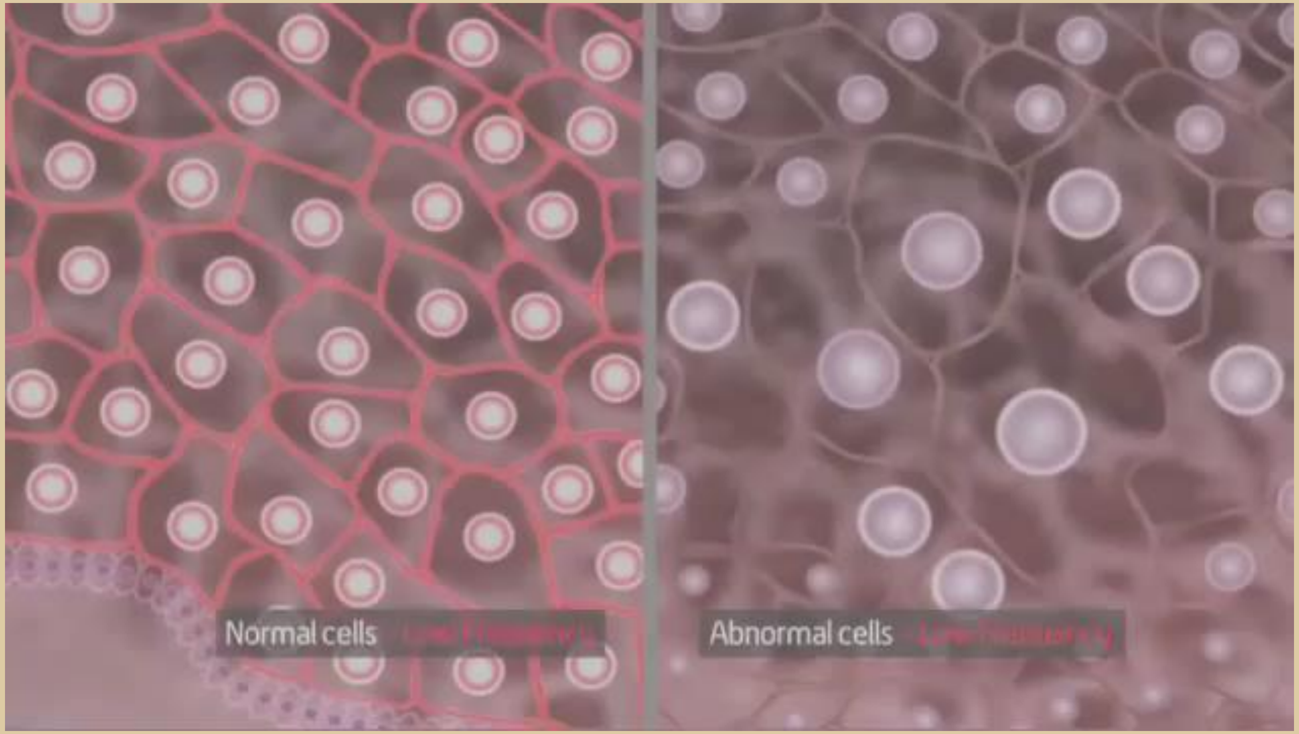

Cell composition and organization are different:

- among different tissue types;
- between normal and abnormal status.

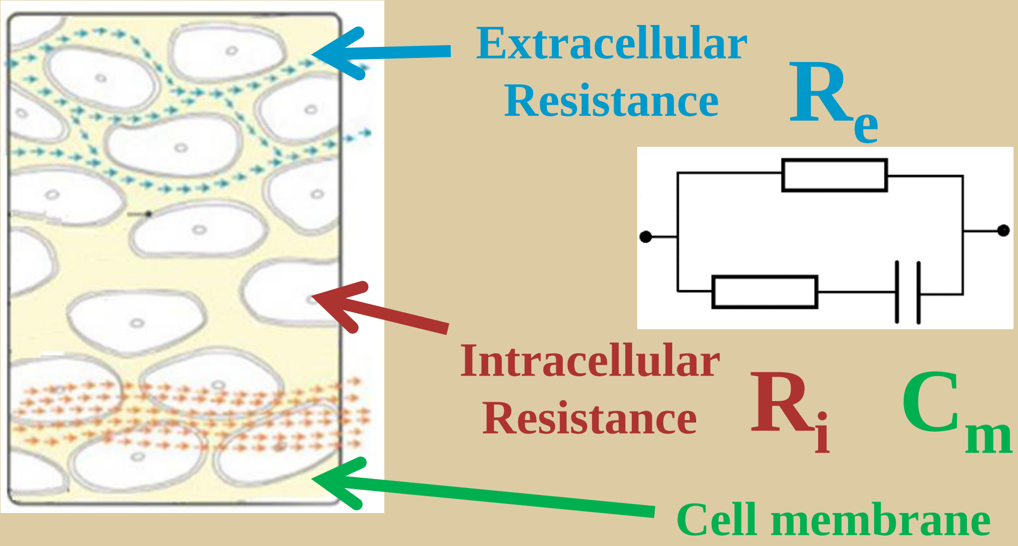

Cole Model

Clinical study

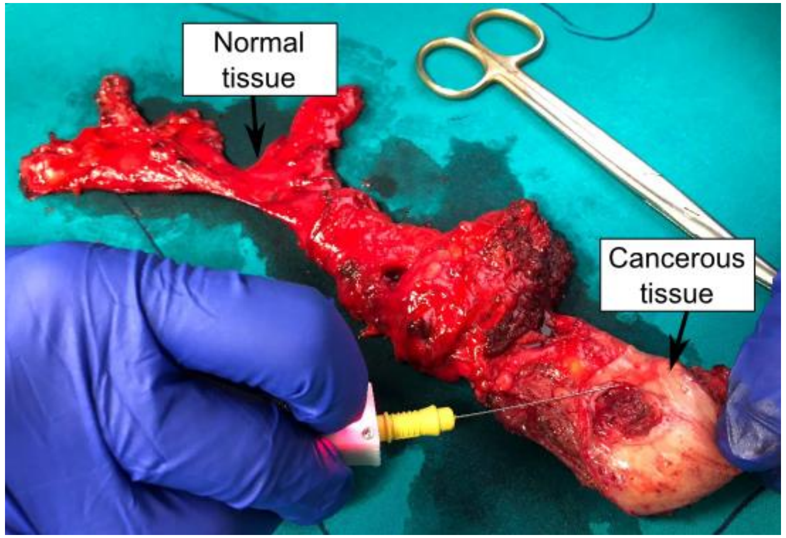

586 data collected from 10 patients:

→Muscle

→Mucosa

→Cartilage

→Salivary Gland

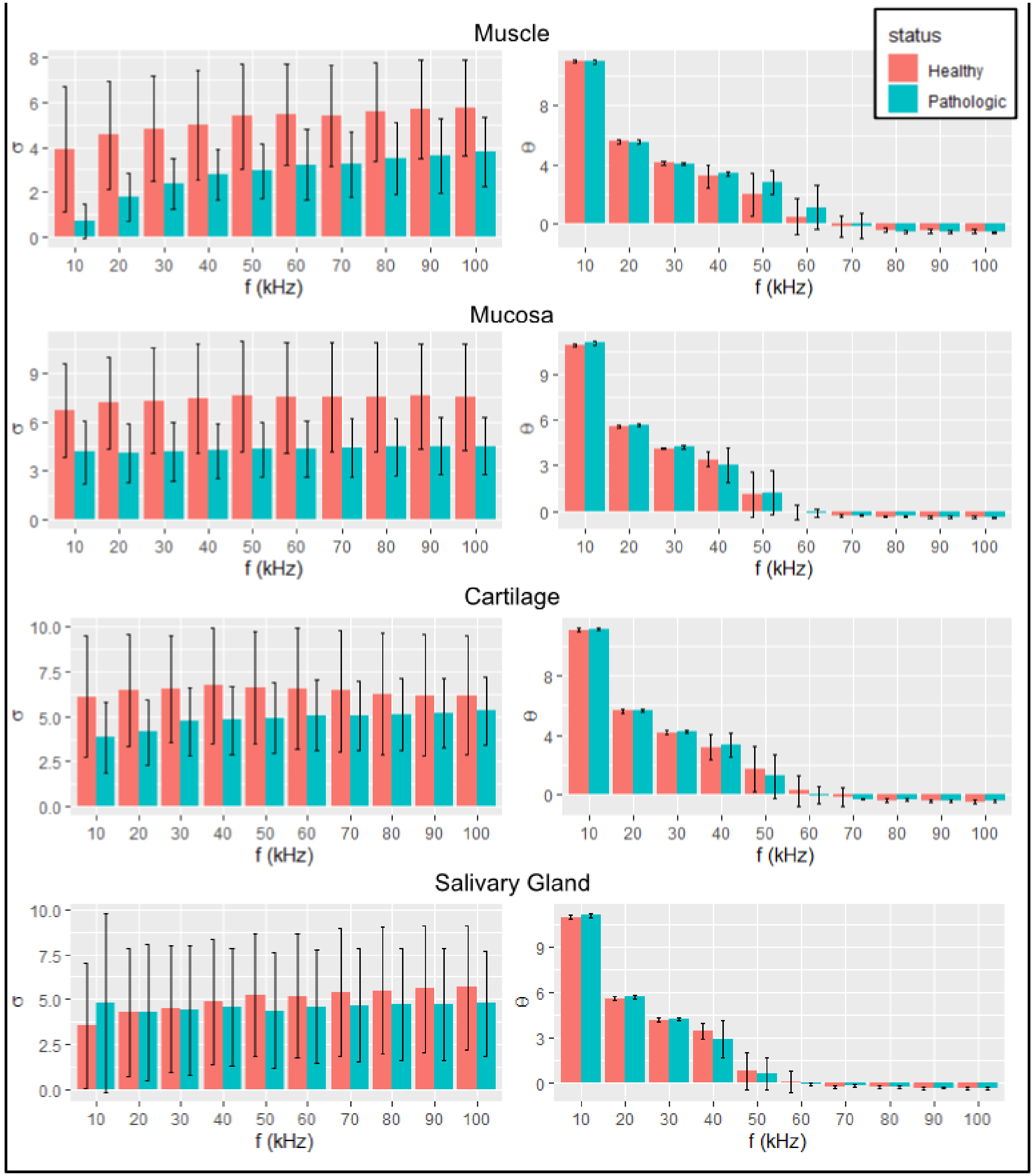

Cheng, Zhuoqi, et al. "SmartProbe: a bioimpedance sensing system for head and neck cancer tissue detection." *Physiological measurement*.

Monopolar & Bipolar

Monopolar configuration

→ Current density: $J_{mono} = \frac{I}{2\pi r^2}$

→ $Z_{mono} = \int_{\Omega} \left(\frac{J_{mono}}{\hat{\sigma}}\right) d\Omega = \frac{1}{2\pi\hat{\sigma}}\left(\frac{1}{r_0} - \frac{1}{r}\right), \quad r \to \infty$

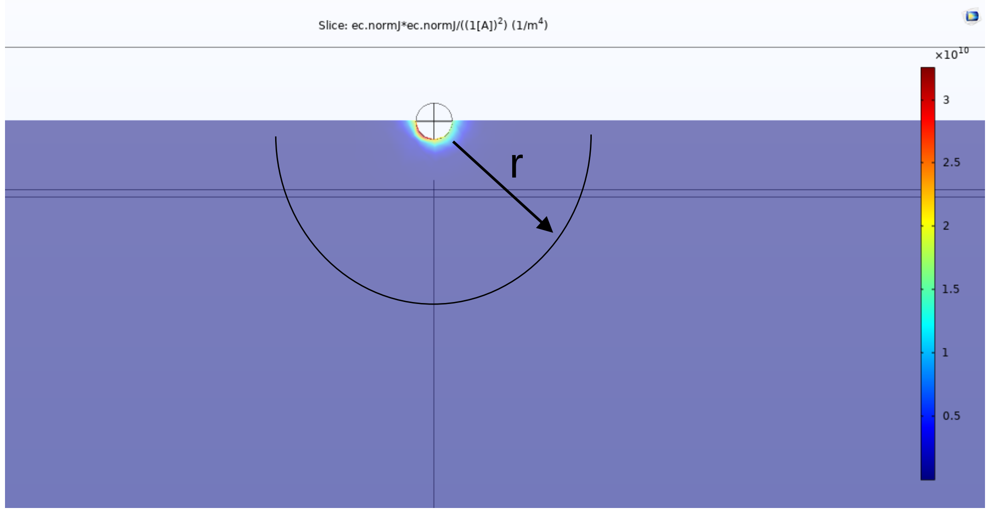

Bipolar configuration

→ $J_{bi} = \frac{I\overrightarrow{AP}}{2\pi|AP|^2} + \frac{I\overrightarrow{BP}}{2\pi|BP|^2}$

→ $Z_{bi} \approx Z_A + Z_B$

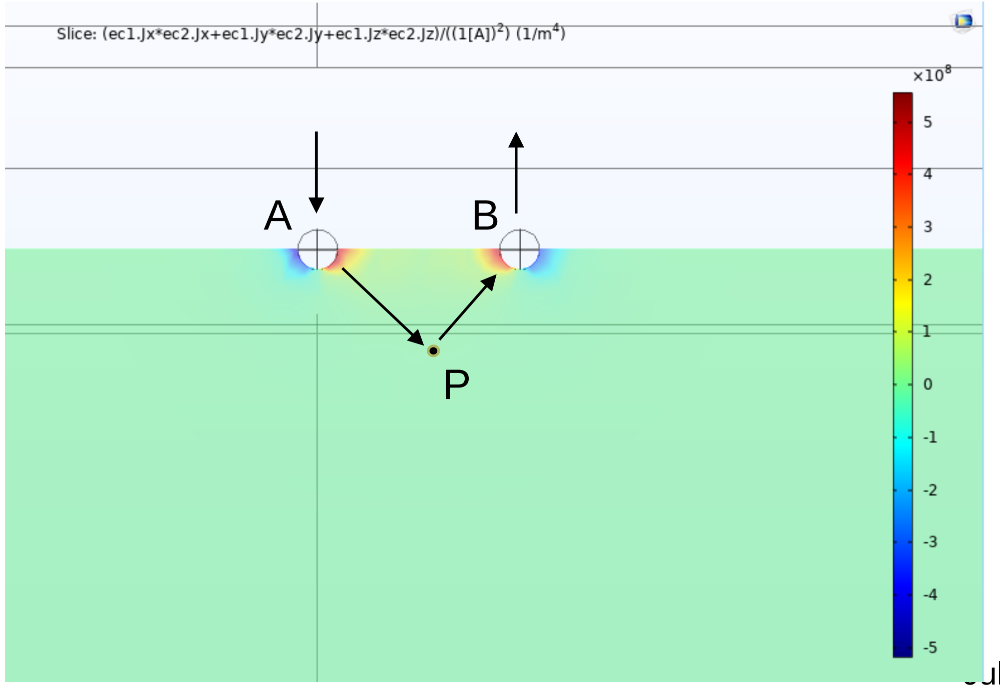

Electric field can be distorted!

Problems and solutions

$$\rightarrow Z_{mono} = \int_{\Omega} \left(\frac{J_{mono}}{\hat{\sigma}}\right) d\Omega = \frac{1}{2\pi\hat{\sigma}} \boxed{\left(\frac{1}{r_0}\right)}$$

→ r_0: the electrode emersed depth matters!

→ Solution:
- → (Robot) Control the electrode emersed depth

→ What if the electrode has an irregular shape:
- → Calibration using standard saline solutions

Monopolar configuration as an example

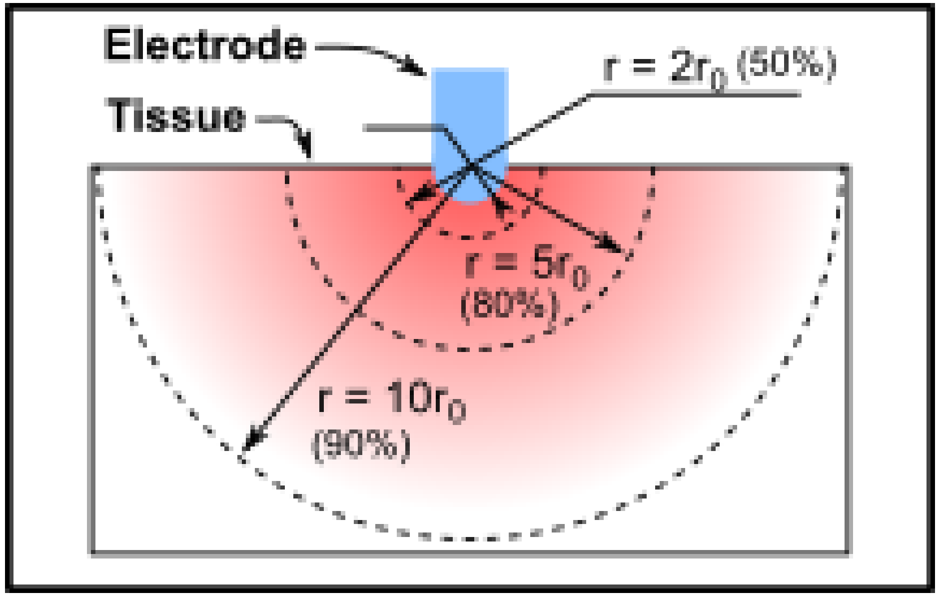

Tripolar configuration

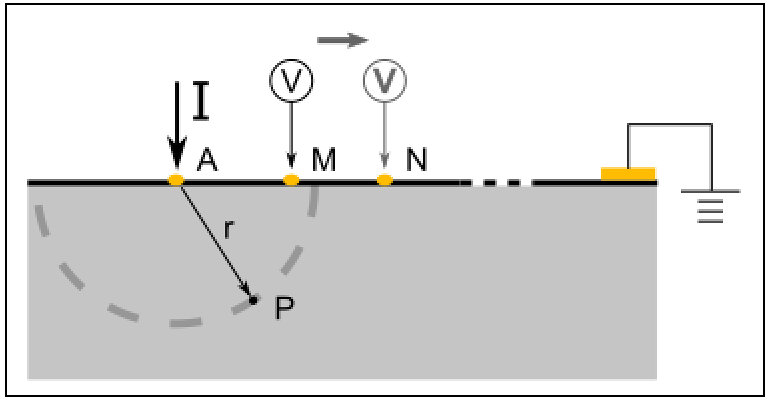

Current density at P: $$J_p = \frac{I}{2\pi r^2}$$

Electric potential at P: $$V_p = \frac{I}{2\pi\sigma}(\frac{1}{r_0} - \frac{1}{r})$$

We measure the electric potential at M & N:

$$V_{MN} = \frac{I}{2\pi\sigma}(\frac{1}{|AM|} - \frac{1}{|AN|})$$

Apparent conductivity:

$$\sigma_a = \frac{I}{2\pi V_{MN}}(\frac{1}{|AM|} - \frac{1}{|AN|})$$

Cheng, Zhuoqi, and Thiusius Rajeeth Savarimuthu. "A novel robot-assisted electrical impedance scanning system for subsurface object detection." *Measurement Science and Technology,* 2021

Pseudo-tetrapolar configuration

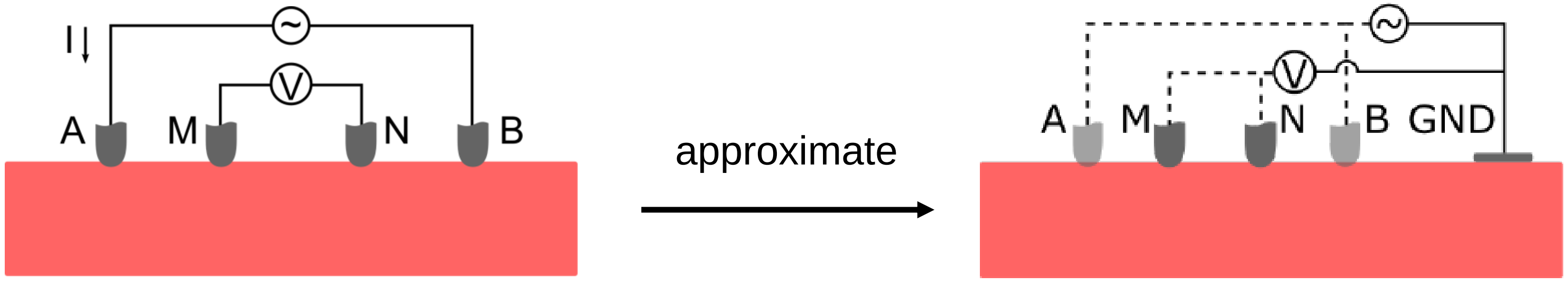

$$Z_{tetra} = Z_{AM} - Z_{AN} - Z_{BM} + Z_{BN} = \frac{1}{2\pi\hat{\sigma}}\left(\frac{1}{|AM|} - \frac{1}{|AN|} - \frac{1}{|BM|} + \frac{1}{|BN|}\right)$$

Useful in robotic surgery due to the limited number of trocars!

Cheng et al. 'Monopolar, Bipolar, Tripolar, and Tetrapolar configurations in Robot Assisted Electrical Impedance Scanning', Biomedical Physics & Engineering Express, 2022

Application Example 1: Robotic peripheral intravenous catheterization

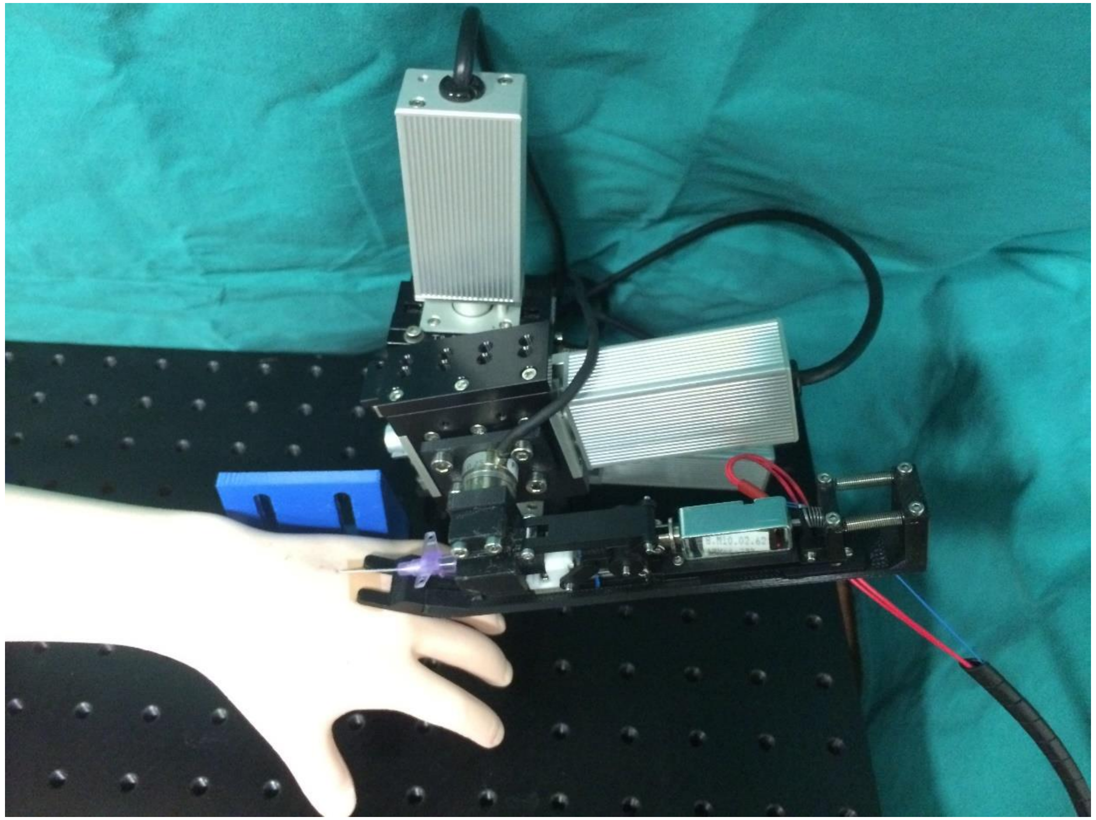

Medical background

The success rates of Peripheral IntraVenous Catheterization (PIVC) are low:

Patient	1 attempt	2 attempts
Adults[11]	72%	
Pediatrics[12]	53%	67%

- Jacobson, et al. ‘Variables influencing intravenous catheter insertion difficulty and failure: an analysis of 339 intravenous catheter insertions.’
- Lininger, et al. ‘Pediatric peripheral IV insertion success rates.’

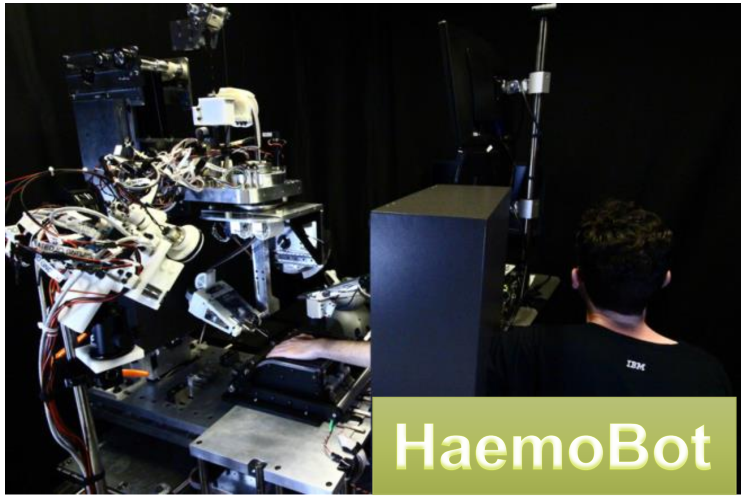

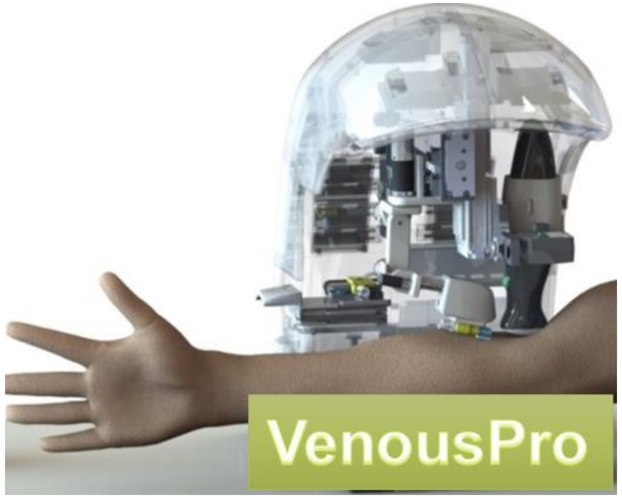

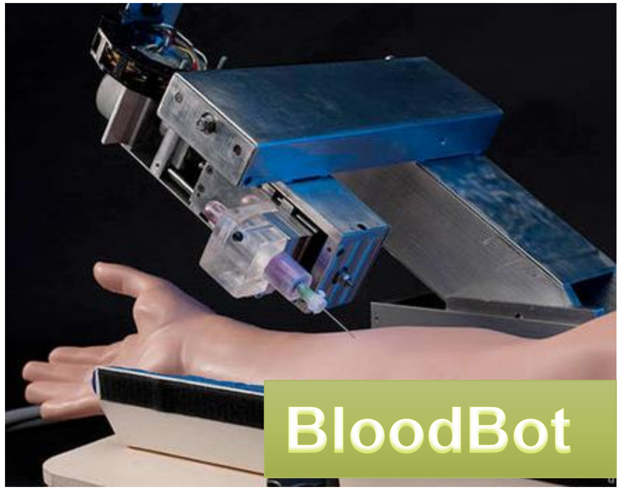

Not suitable for pediatric patients!

Hand-held robotic device for PIVC on pediatric patients

Advantages:

- Keeping surgeons in control;
- Flexible insertion sites;
- High acceptance rate;
- Low cost and complexity.

Detect venipuncture using EBI

Bipolar configuration

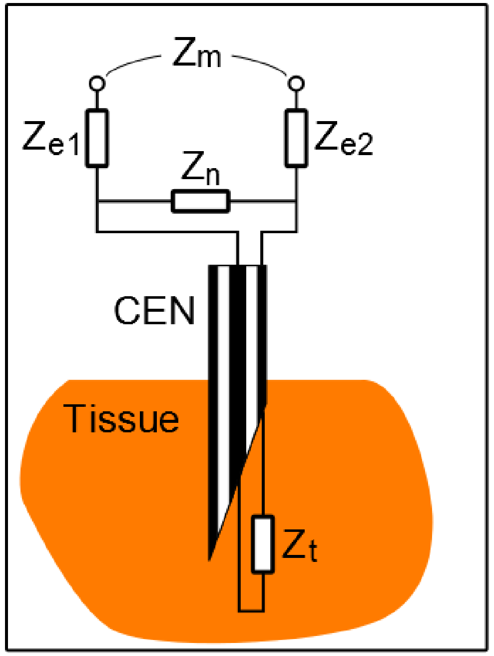

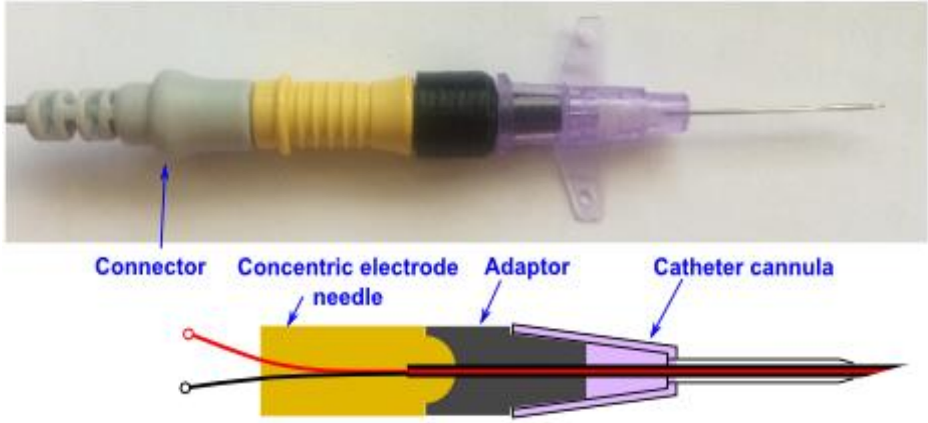

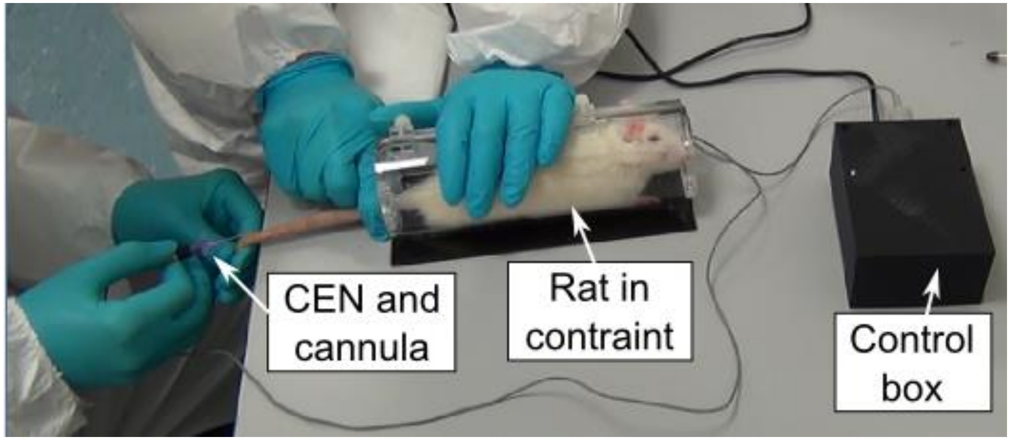

Z_{e1} and Z_{e2}: the impedance of the electrodes;
Z_n: the electrical impedance due to the capacitance effect between the electrodes.
Z_t: the electrical impedance of bio-tissue.
Z_m: the measured electrical impedance of the equivalent circuit.

$$\begin{cases} R_t = \frac{R_m(R_n^2+X_n^2)-R_n(R_m^2+X_m^2)}{(R_n-R_m)^2+(X_n-X_m)^2} \\ X_t = \frac{X_m(R_n^2+X_n^2)-X_n(R_m^2+X_m^2)}{(R_n-R_m)^2+(X_n-X_m)^2} \end{cases}$$

The electrical impedance values are interpreted in a format of a real part R (resistance) and an imaginary part X (reactance).

$$Z_t = R_t + jX_t$$

Z. Cheng, B. L. Davies, D. G. Caldwell and L. S. Mattos, A new venous entry detection method based on electrical impedance sensing, Annals of Biomedical Engineering.

Data processing and analysis

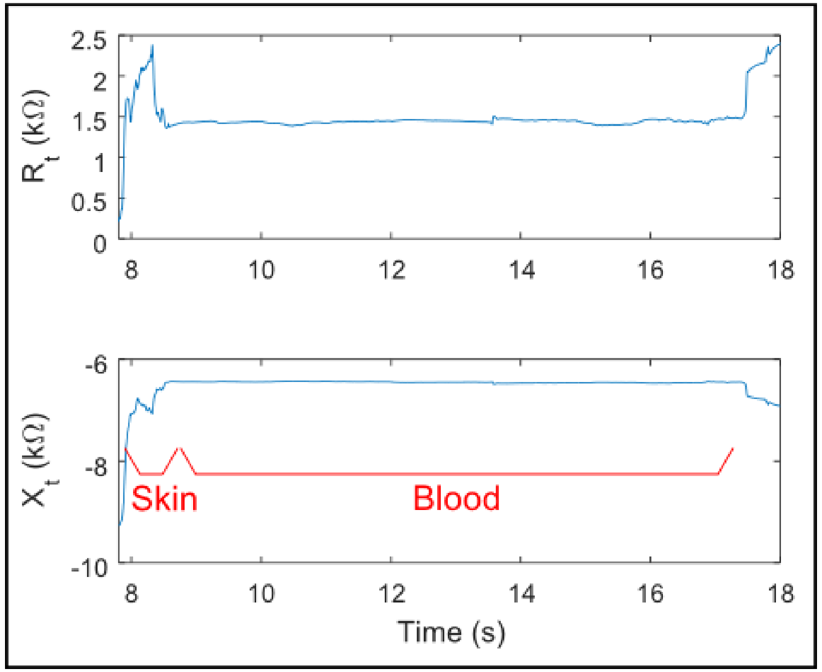

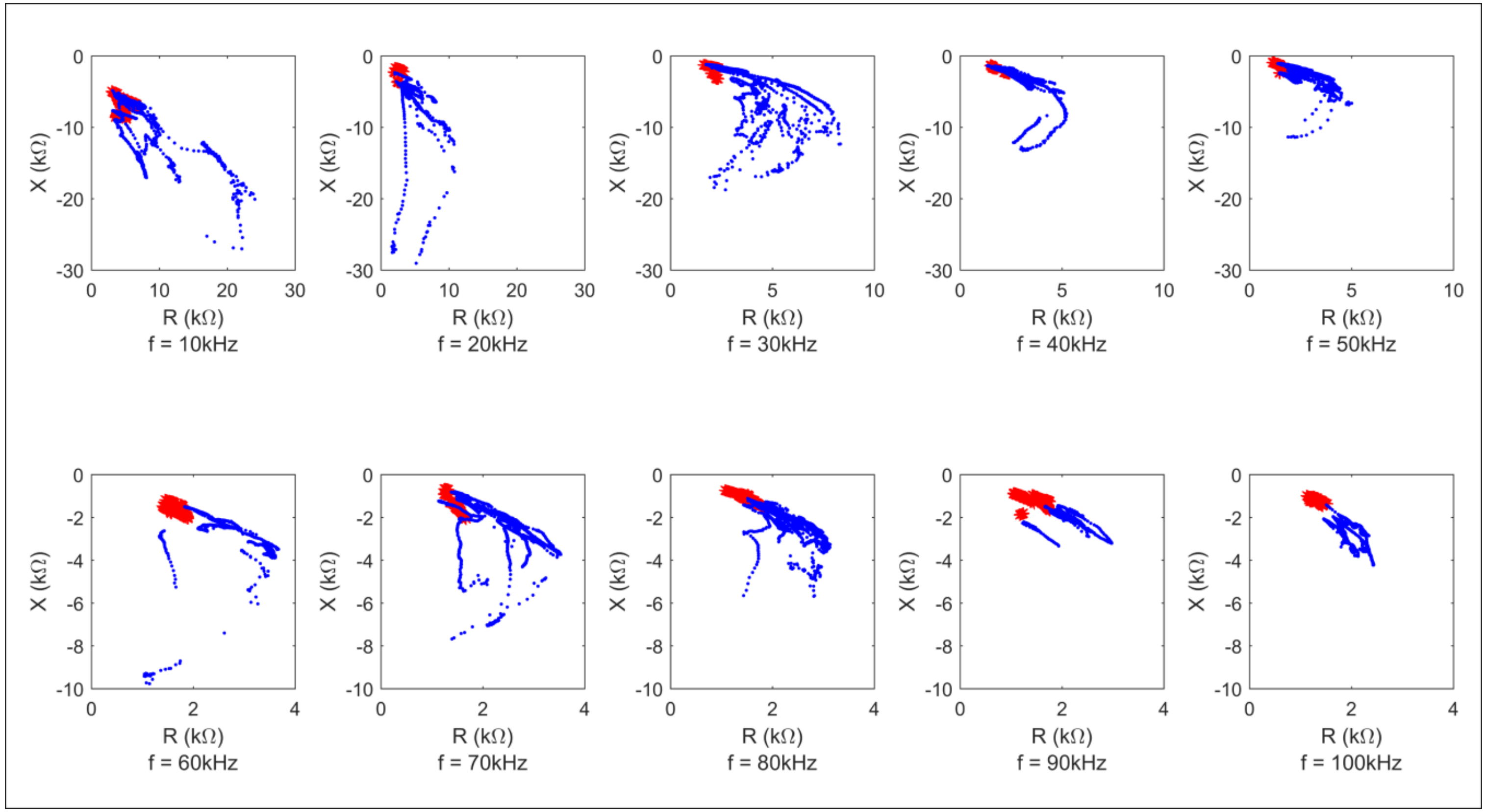

f (kHz)	10	20	30	40	50	60	70	80	90	100
DT	87.5%	98.3%	92.8%	95.1%	95.1%	100%	89.4%	97.7%	99.4%	100%
LD	74.5%	88.3%	83.8%	88.7%	88.5%	95.9%	78.7%	84.9%	98.2%	99.3%
SVM	74.7%	95.5%	88.2%	89.3%	89.6%	98.2%	82.8%	92.1%	98.6%	100%

DT: Decision tree; LD: Linear discriminant; SVM: Support Vector Machine.

Handheld robotic devices

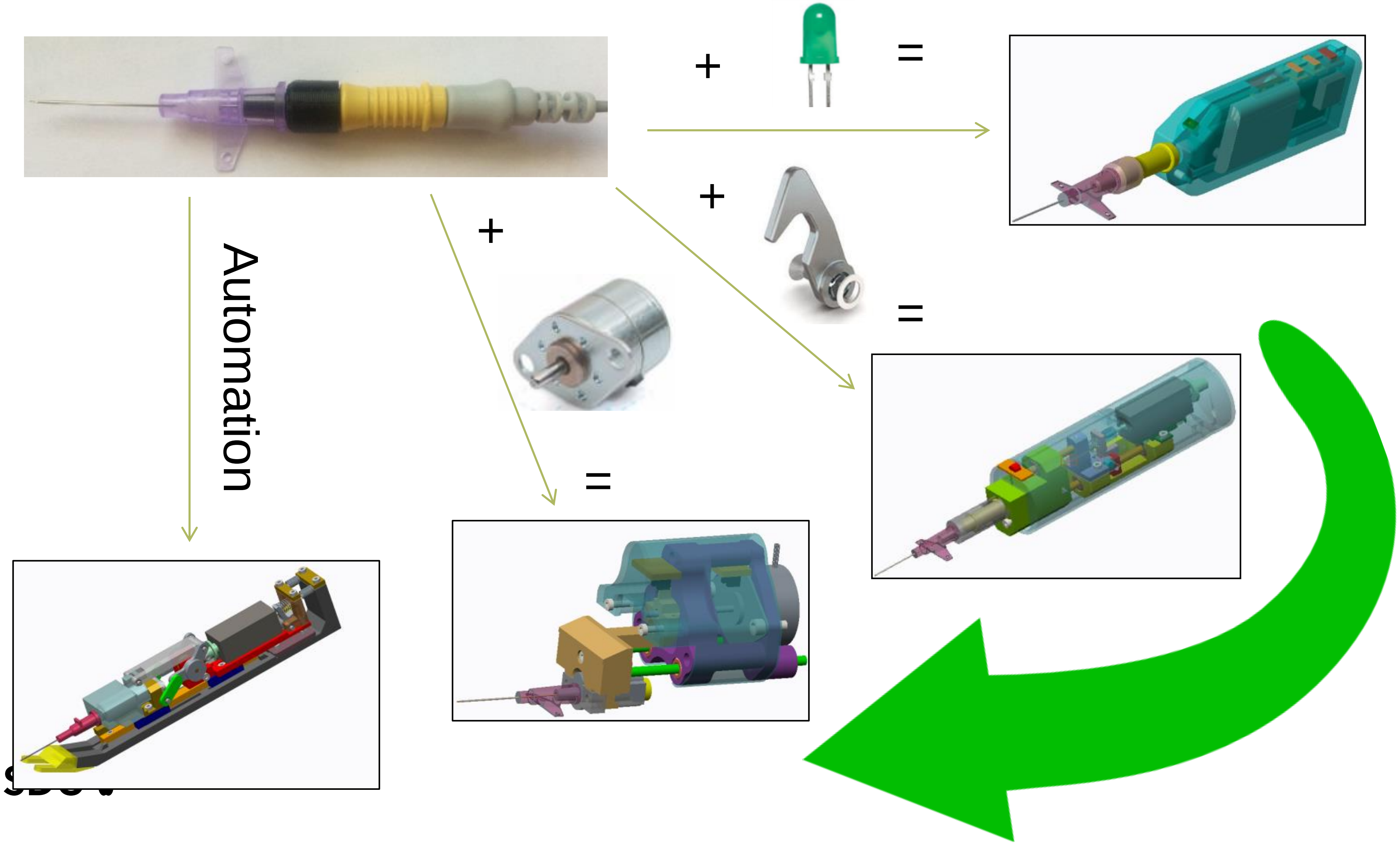

- Mechanism:
  simple -> complex

- The **control** and **responsibility** shared by the operator decrease.

Device 1: sensor only device

SVEI: Smart Venous Entry Indicator

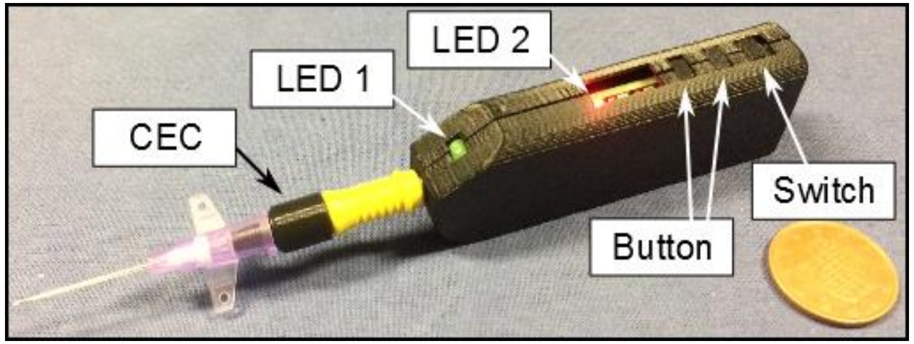

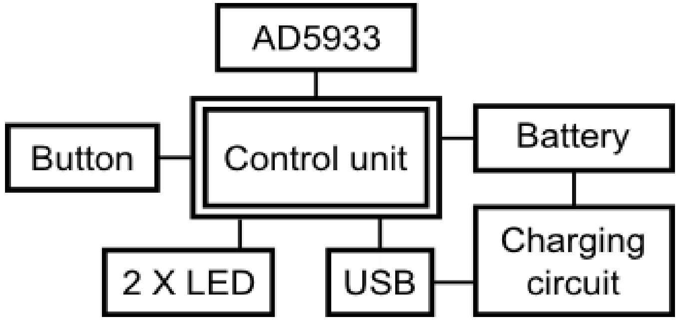

Z. Cheng, B. L. Davies, D. G. Caldwell and L. S. Mattos, ‘A NEW VENOUS ENTRY DETECTION METHOD BASED ON ELECTRICAL BIO-IMPEDANCE SENSING,’ Annals of Biomedical Engineering

Device 2: Disengage device

SDOP: Smart Device for Over puncture Prevention

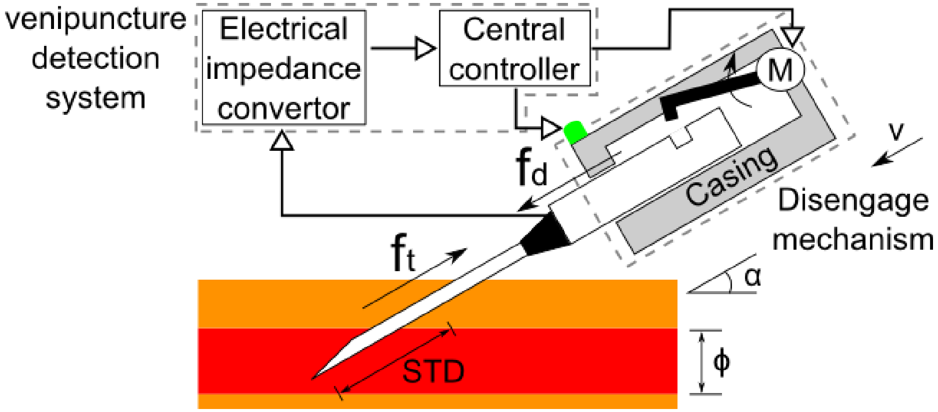

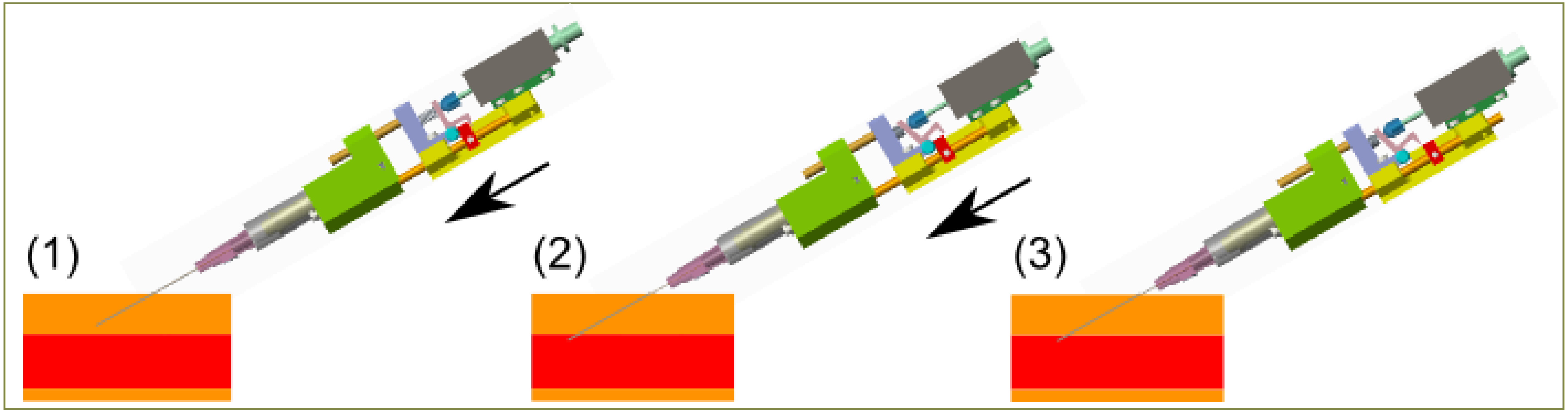

Z. Cheng, B. L. Davies, D. G. Caldwell and L. S. Mattos, SDOP: A Smart handheld Device for Over puncture Prevention during pediatric peripheral intravenous catheterization.

Device 3: Motorized insertion

SAID: Semi-Autonomous Intravenous access Device

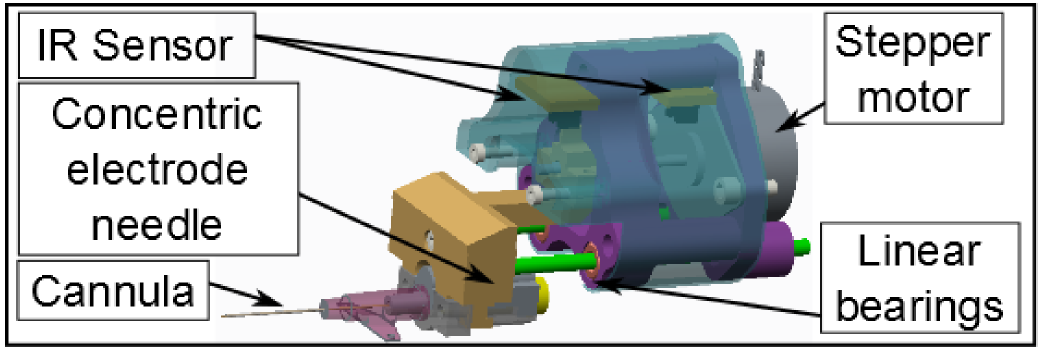

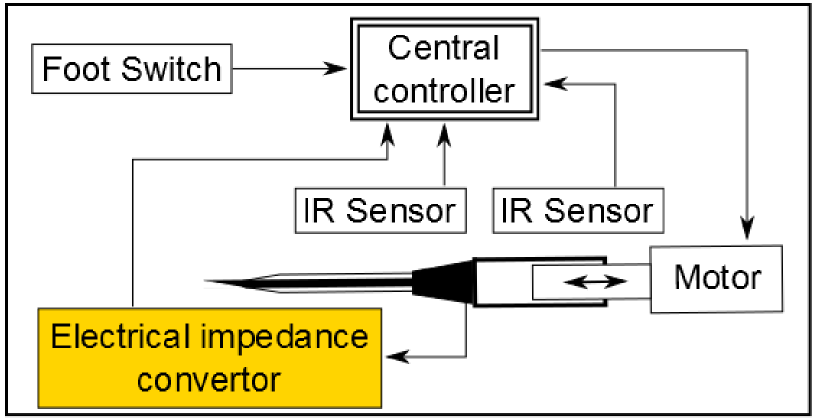

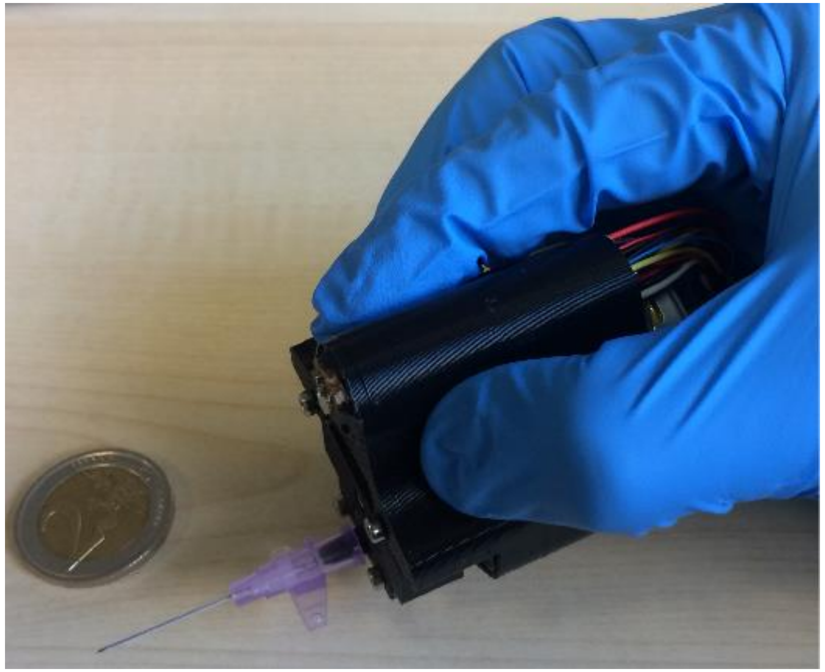

Z. Cheng, B. L. Davies, D. G. Caldwell, G. Barresi, Q. Xu and L. S. Mattos, A hand-held robotic device for peripheral intravenous catheterization, Journal of Engineering in Medicine

Device 4: Handheld automation solution

CathBot

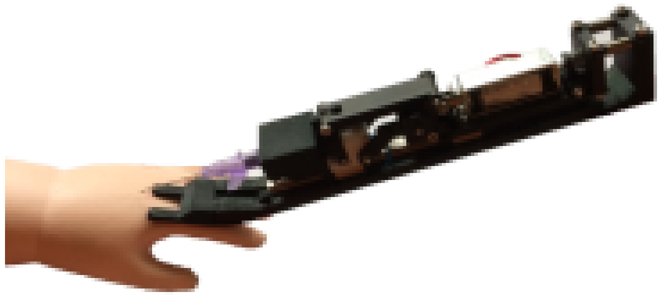

The user only needs to push the handle forwards.

The device:
1. Insert the catheter;
2. Stop the insertion after venipuncture;
3. Advance the catheter 1 mm further;
4. Advance the cannula but retract the needle.

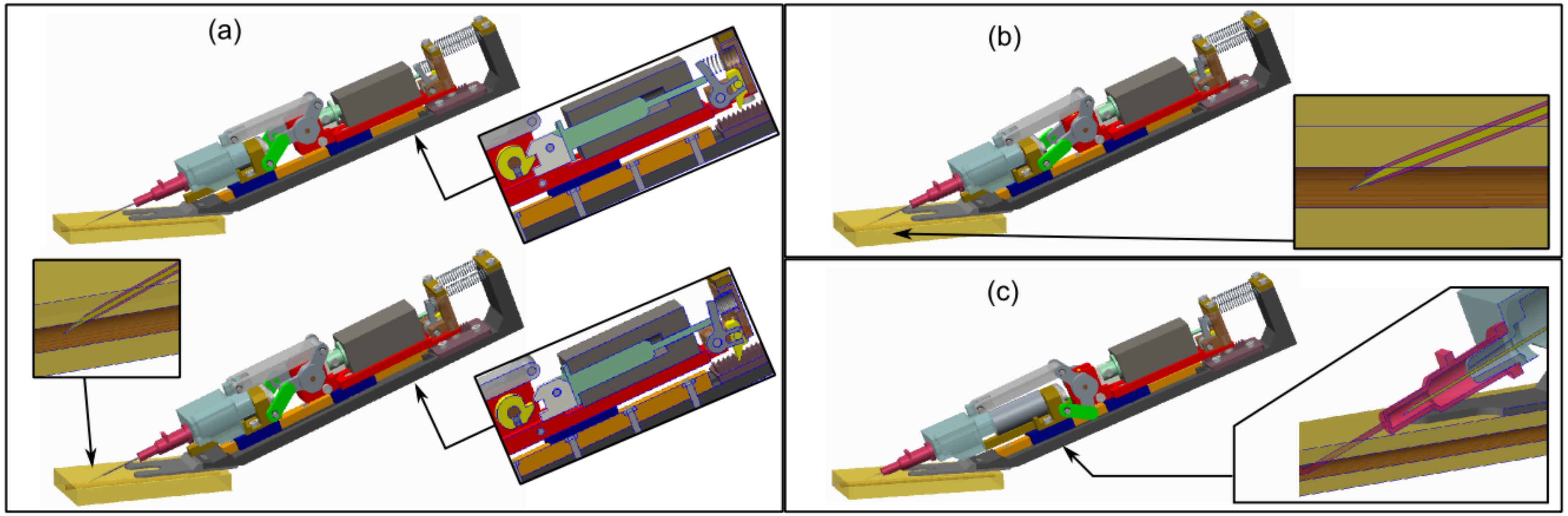

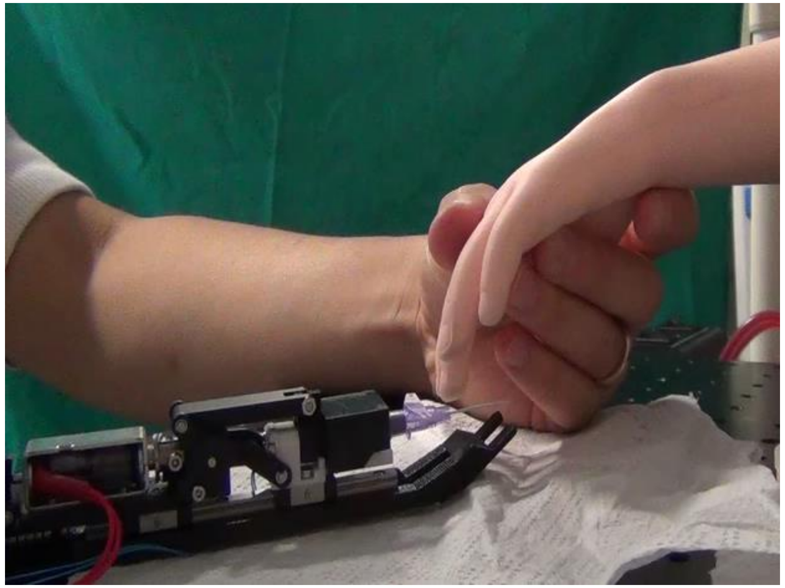

Experimental results comparing 5 methods

Compare 5 devices:

- Evaluates the handheld device with the realistic baby arm phantom.
- 25 naïve subjects (no experiences of PIVC or needle insertion) were invited to the experiment.
- Each subject did 10 attempts on the phantom using one of the devices.

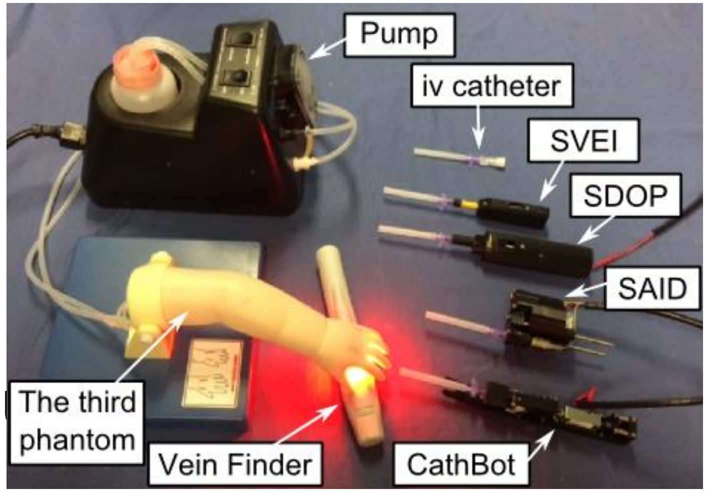

Device	Name	Ave. success rat	1st stick accuracy	Whole operation time	SUS score
	SVEI	86%±15%	5/5	23,9 s	77,8
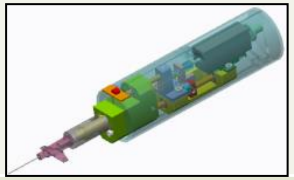	SDOP	78%±14,7%	2/5	18,8 s	81,5
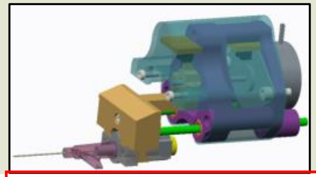	SAID	80%±17%	3/5	19 s	75,8
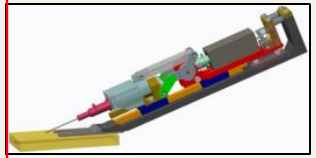	CathBot	84%±8%	4/5	16,9 s	72,8
	Conventional	12%±16%	0/5	36,2 s	NA

Application Example 2:
Robot Assisted Electrical Impedance Sensing
(RAEIS)

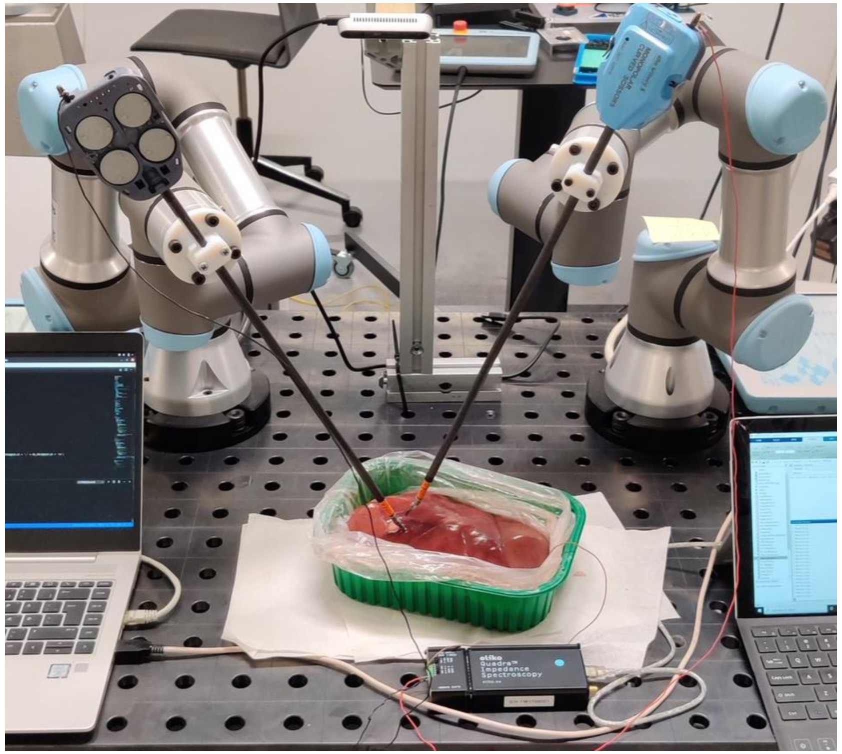

Tissue recognition in Robot Assisted Minimally Invasive Surgery (RAMIS)

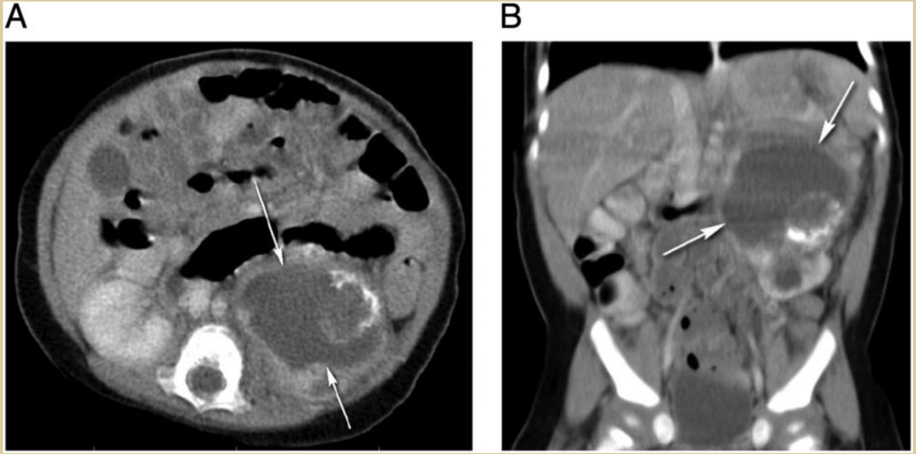

register

Higher level of perception & recognition for autonomous surgery tomorrow!

Constraints in RAMIS:

- Number of trocars
- Small workspace
- Robotic maneuverability
- Surgical workflow

<u>Sensing system built upon the existing surgical robotic instruments & system</u>

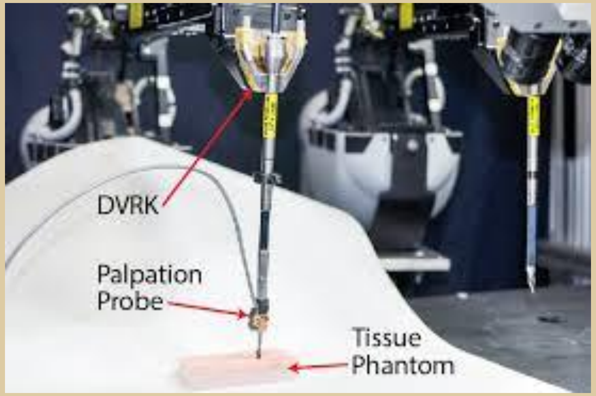

Robot-Assisted Electrical Impedance Sensing (RAEIS)

Mobile electrodes controlled by robots to multiple positions for impedance sensing.

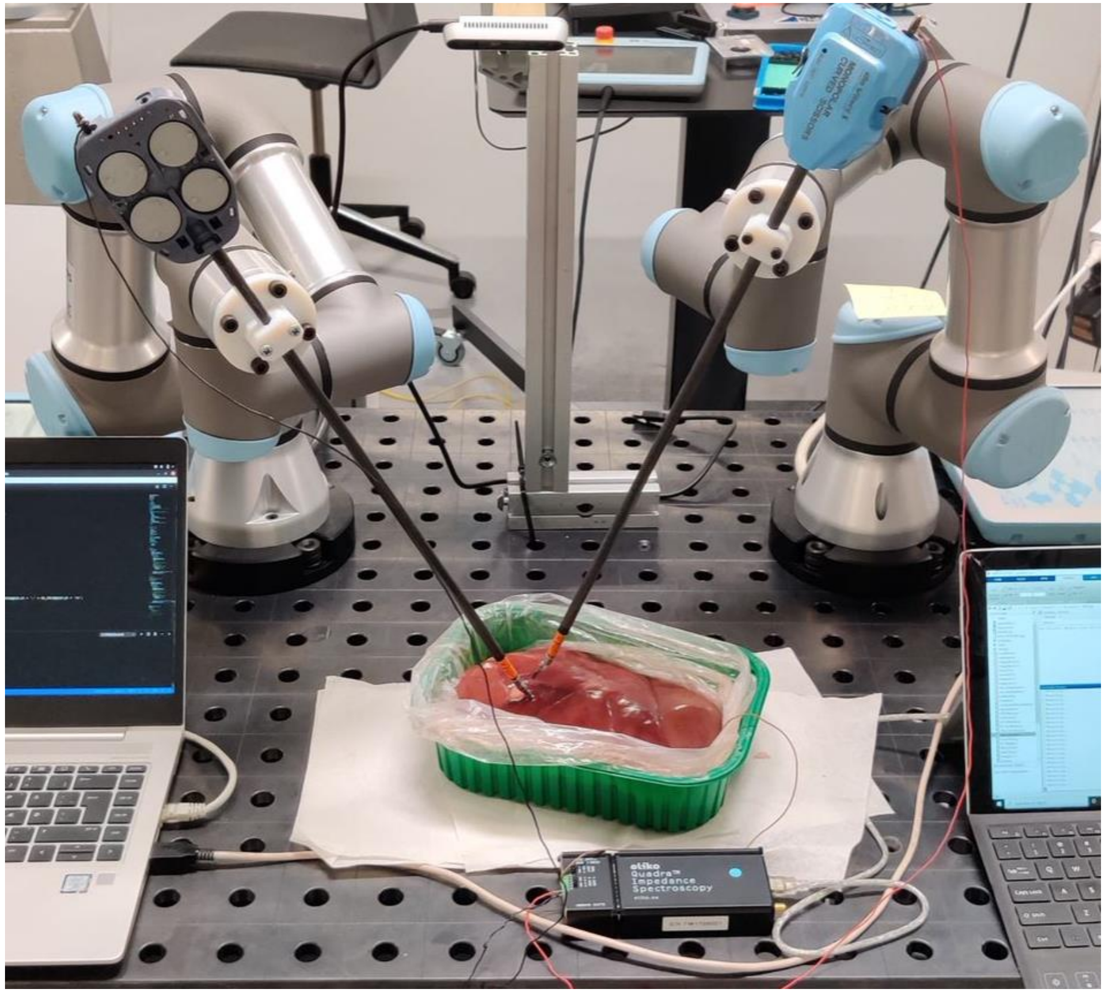

Advantages:

- No external devices involved to the surgical site
- Flexible and autonomous sensing
- Fast and accurate tissue identification

Monopolar configuration

→ The key is the electrode's pressing depth

→ Impedance:

$$Z_{mono} = \int_{\Omega} \left(\frac{J_{mono}}{\hat{\sigma}}\right) d\Omega = \frac{1}{2\pi\hat{\sigma}}\left(\frac{1}{r} - \frac{1}{r_0}\right)$$

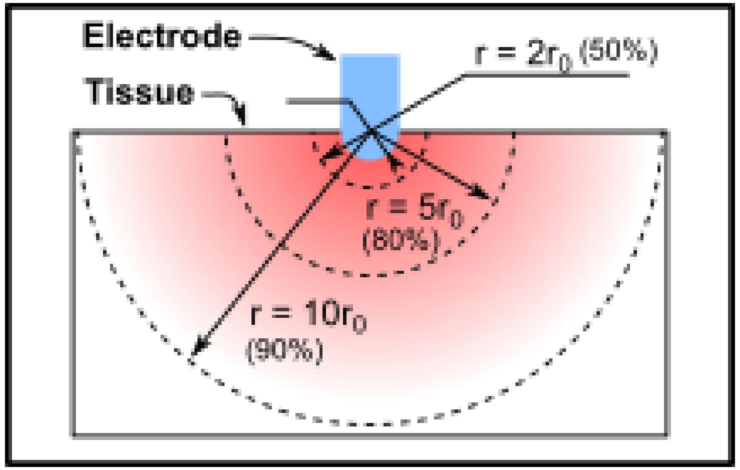

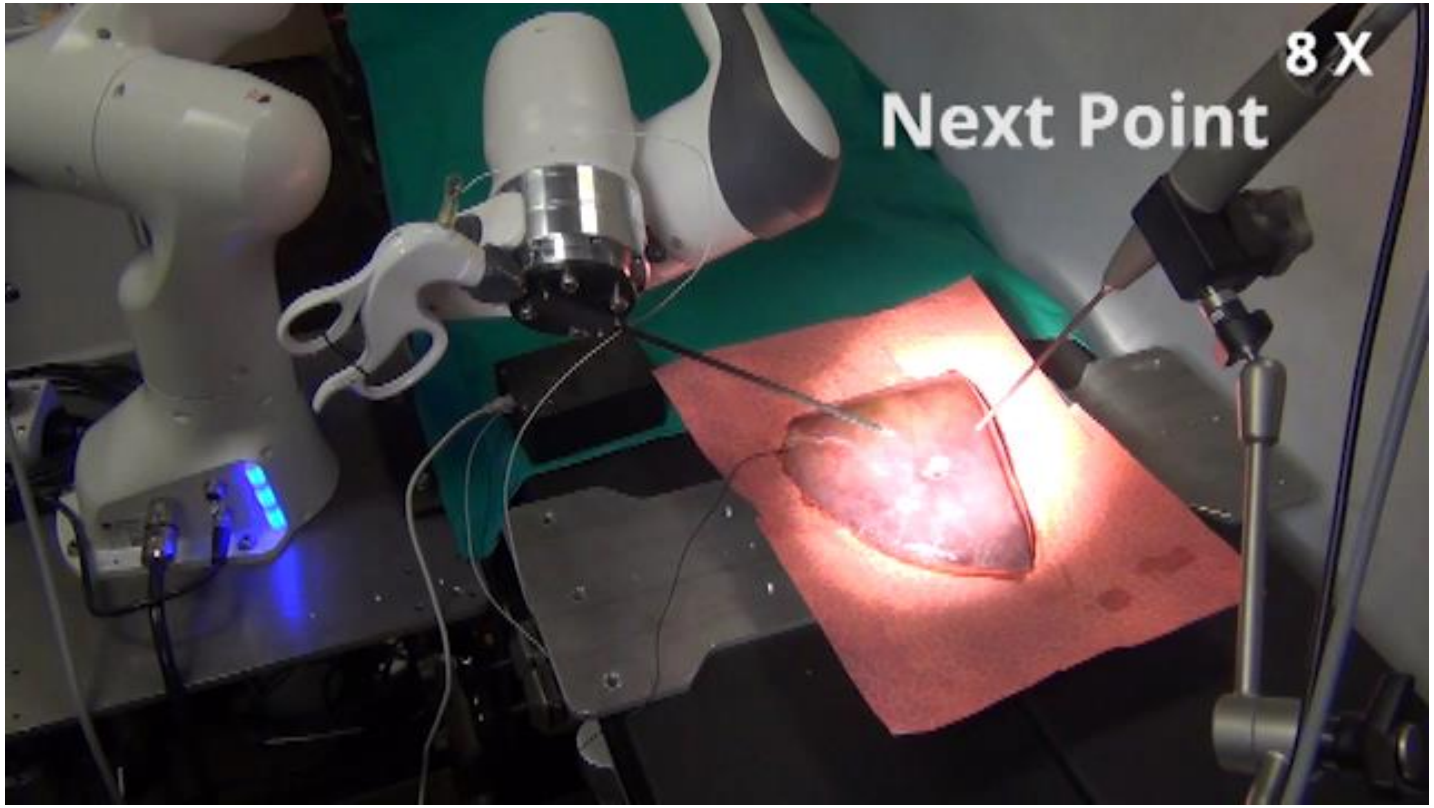

Penza, V.*, Cheng, Z.*, Koskinopoulou, M., Acemoglu, A., Caldwell, D. G., & Mattos, L. S. "Vision-guided Autonomous Robotic Electrical Bio-Impedance Scanning System for Abnormal Tissue Detection." IEEE Transactions on Medical Robotics and Bionics.

Bipolar configuration

→ Assuming that bipolar is achieved by 2 jaws: A and B

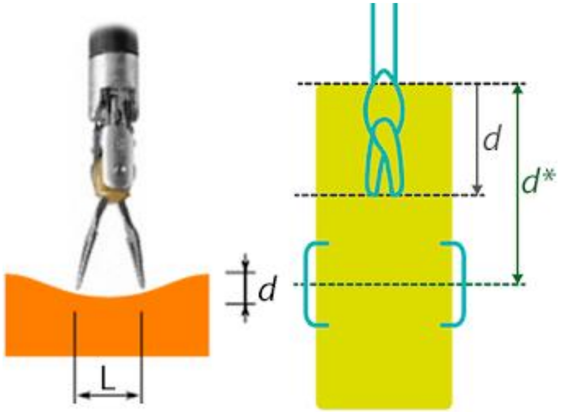

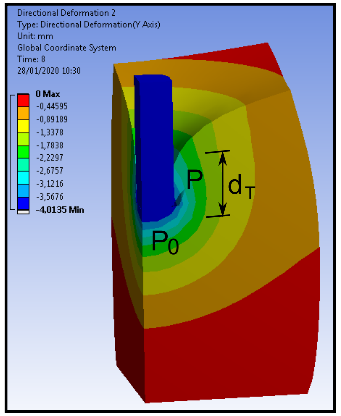

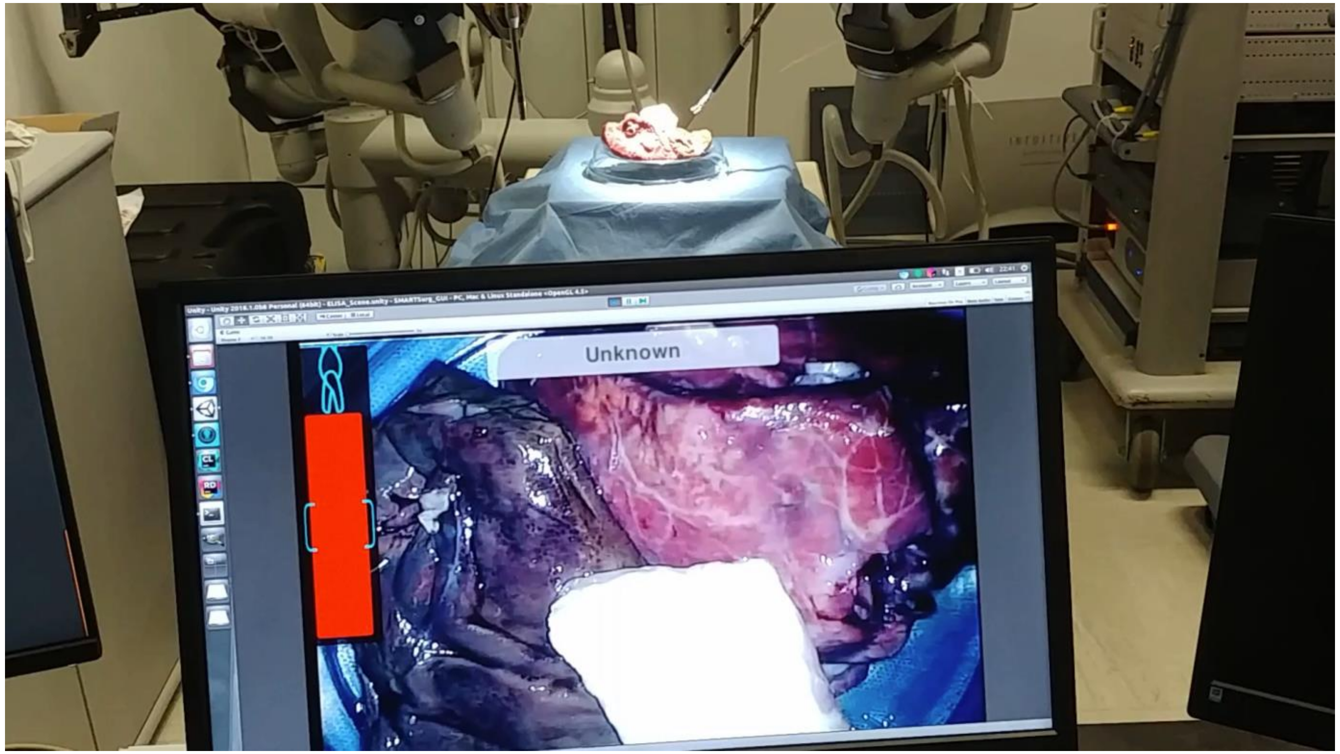

Zhuoqi Cheng, Diego Dall'Alba, Simone Foti, Andrea Mariani, Thibaud Jean Eudes Chupin, Darwin Gordon Caldwell, Giancarlo Ferrigno, Elena De Momi, Leonardo S Mattos, and Paolo Fiorini. Design and integration of electrical bio-impedance sensing in surgical robotic tools for tissue identification and display. Frontiers in Robotics and AI, 2019.

Tripolar sensing configuration

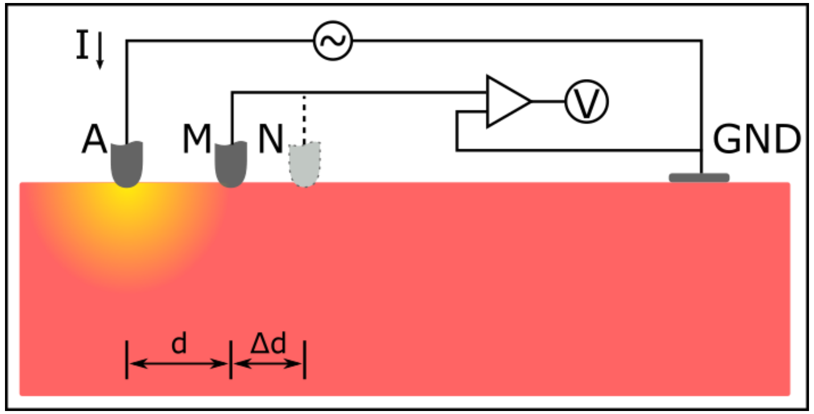

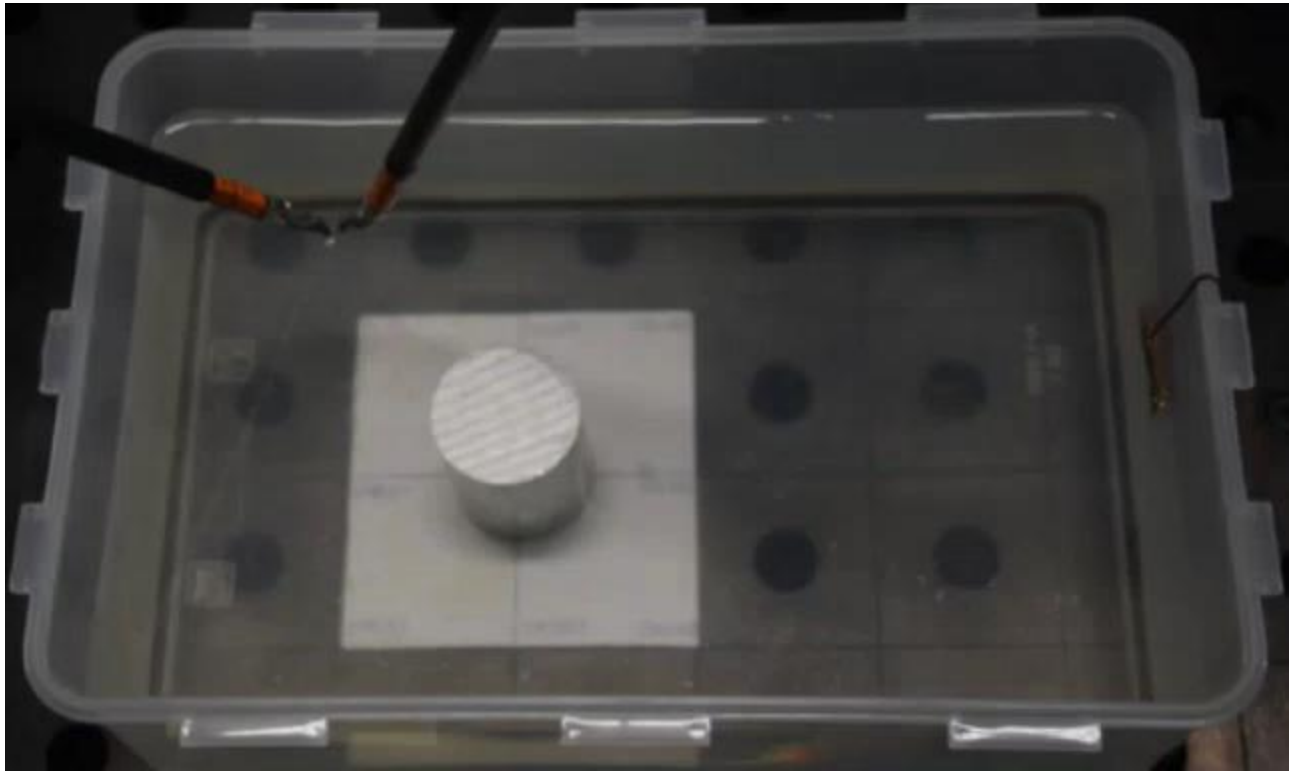

Advantages compared to mono/bipolar:

- Insensitive to electrode emersed depth
- Measured material conductivity accurately
- Detect subsurface region

Cheng, Zhuoqi, and Thiusius Rajeeth Savarimuthu. "A novel robot-assisted electrical impedance scanning system for subsurface object detection." *Measurement Science and Technology,* 2021

System characterization

The system was tested using different saline solutions (0.1%, 0.2%, and 0.3%)

Emersed depths of electrodes (h=1mm and 2mm)

$$\begin{cases} \sigma = \frac{1}{2\pi} \frac{Re_{MN}}{Re_{MN}^2 + Im_{MN}^2} \left(\frac{1}{AM} - \frac{1}{AN}\right) \\ \varepsilon_r = \frac{1}{4\pi^2 f \varepsilon_0} \frac{Im_{MN}}{Re_{MN}^2 + Im_{MN}^2} \left(\frac{1}{AM} - \frac{1}{AN}\right) \end{cases}$$

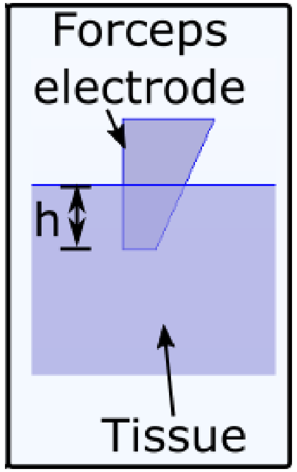

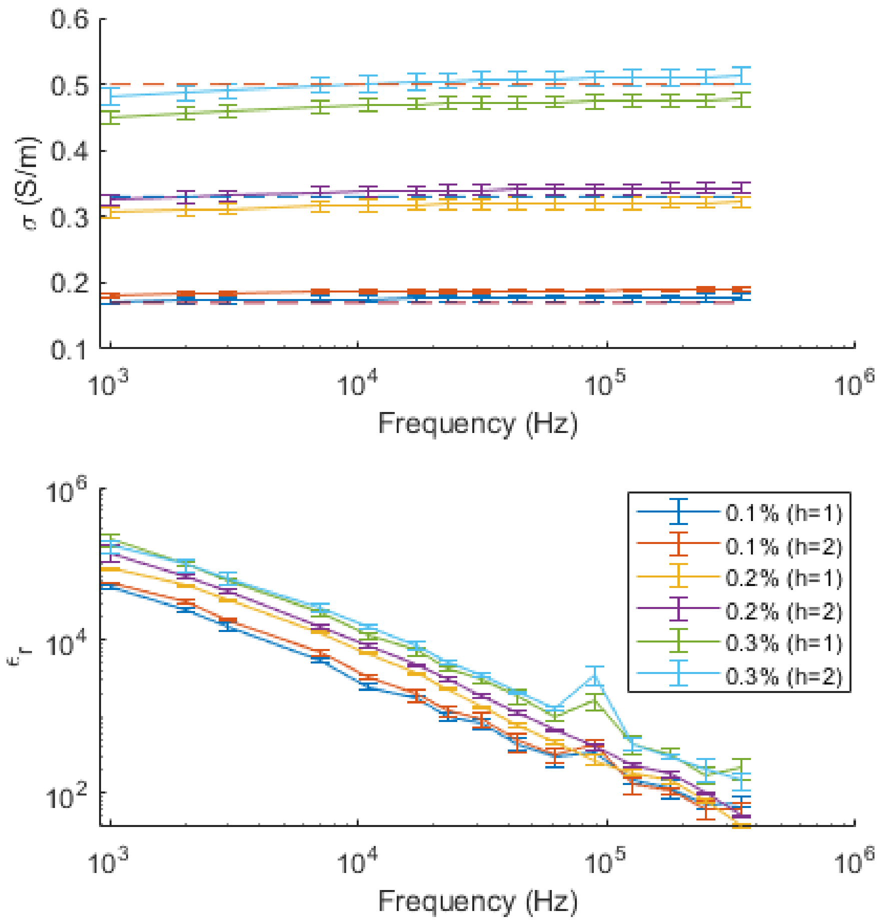

Cheng, Zhuoqi, et al. "Robot Assisted Electrical Impedance Scanning for tissue bioimpedance spectroscopy measurement." *Measurement*.

System characterization

Different ex vivo tissues:

- Porcine liver
- Porcine fat
- Porcine muscle
- Chicken muscle
- Bovine muscle

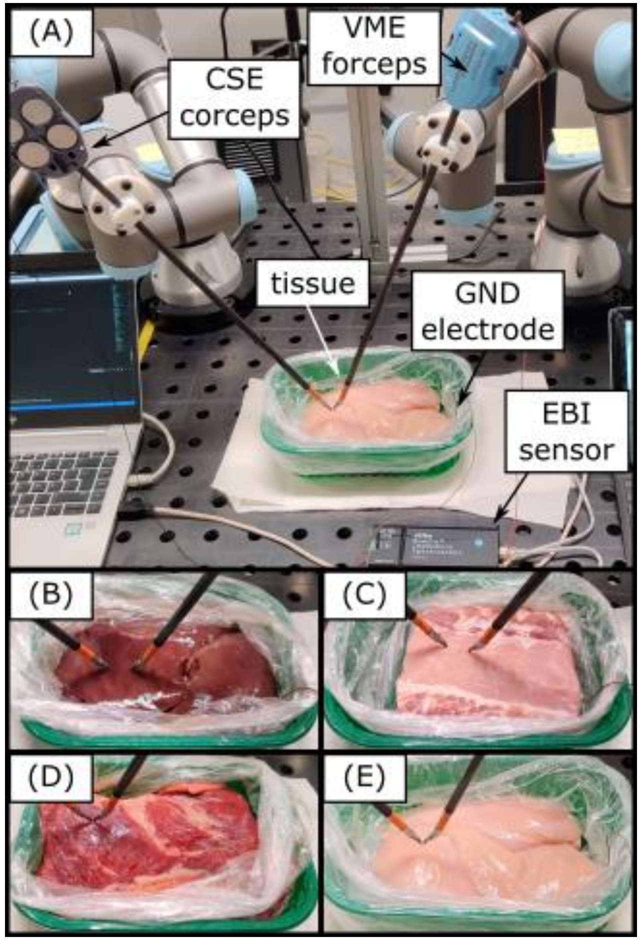

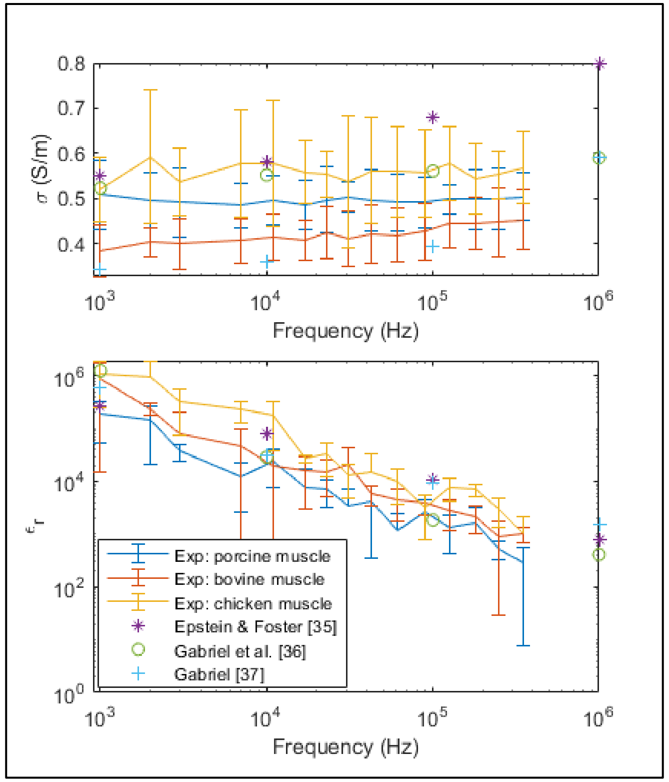

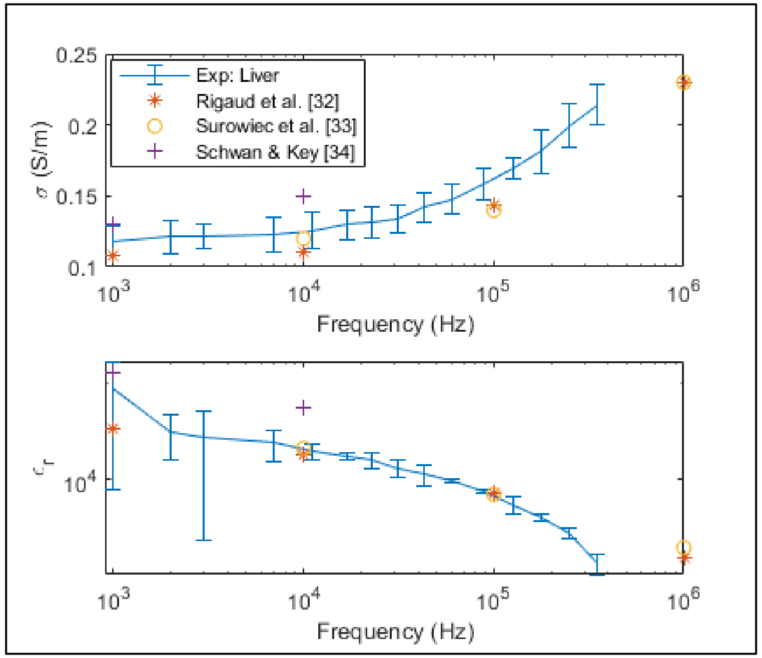

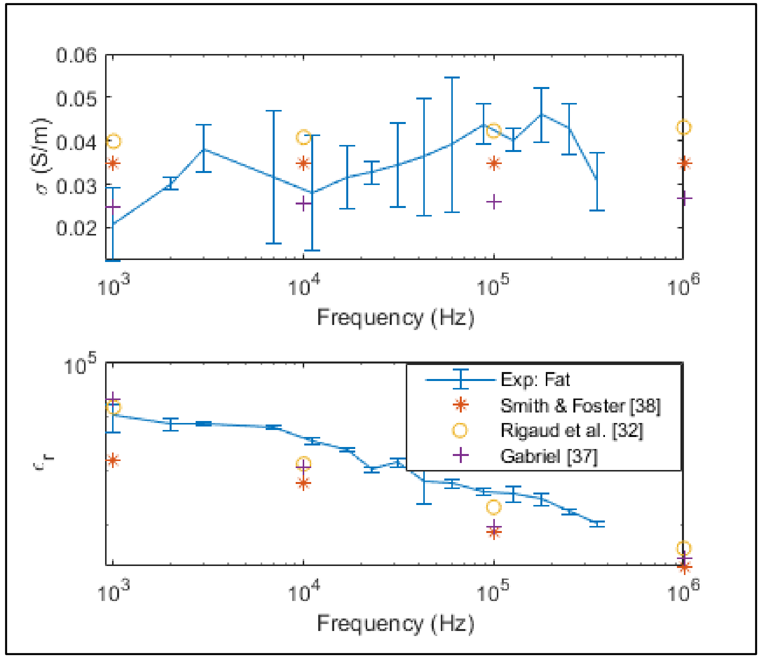

Cheng, Zhuoqi, et al. "Robot Assisted Electrical Impedance Scanning for tissue bioimpedance spectroscopy measurement." Measurement. 2022

Subsurface object detection

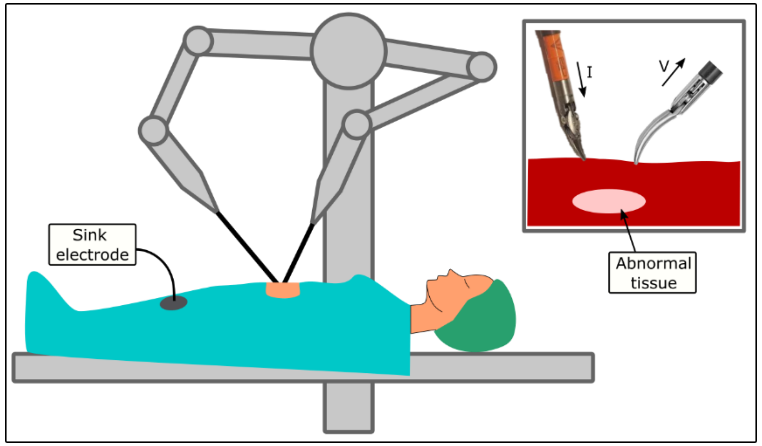

- Early stage cancer
- Lymph nodes
- Blood vessels
- Edema
- etc

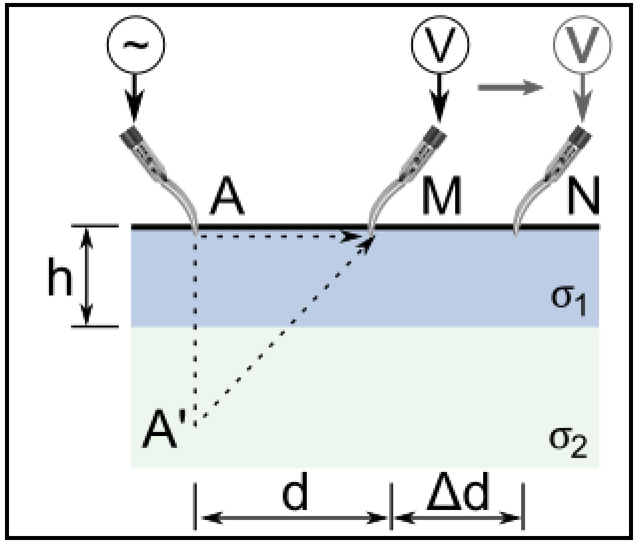

If the object is constructed by 2 layers: ρ_1 and ρ_2

$$V_M^* = \frac{I}{2\pi\sigma_1}\left(\boxed{\frac{1}{d}} + 2\boxed{\sum_{n=1}^{\infty}\frac{\kappa^n}{\sqrt{d^2+(2nh)^2}}} - \frac{1}{r_0}\right)$$

flow from A to M reflected from the interface

Reflection coefficient κ: $\kappa = \frac{\sigma_1 - \sigma_2}{\sigma_1 + \sigma_2}$

Updated voltage calculation:

$$V_{MN}^* = \frac{I}{2\pi\sigma_1}\left(\frac{\Delta d}{d(d+\Delta d)} + \boxed{2\sum_{n=1}^{\infty}\left(\frac{k^n}{\sqrt{d^2+(2nh)^2}} - \frac{k^n}{\sqrt{(d+\Delta d)^2+(2nh)^2}}\right)}\right)$$

=0 if there is no subsurface object

Subsurface object imaging

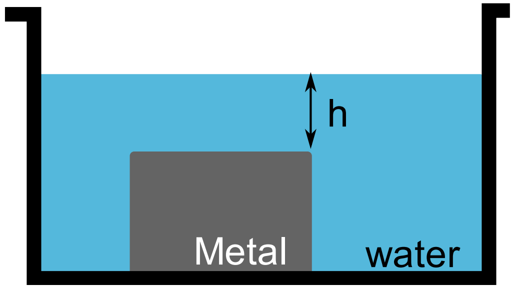

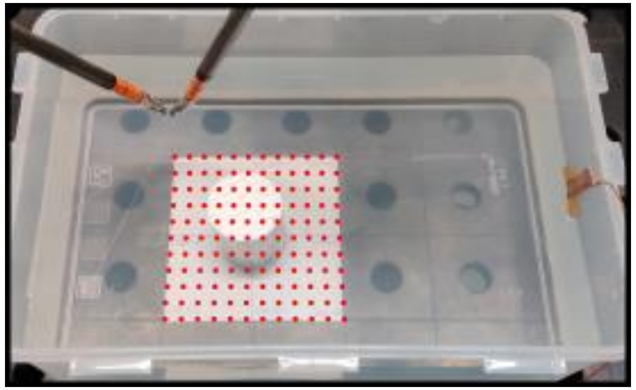

Scanning area: (100mm*100mm)
Scanning resolution: 11*11
metal cylinder diameter: 40mm

Two conditions (Immersed depth of the metal object:
1) h=5mm
2) h=10mm

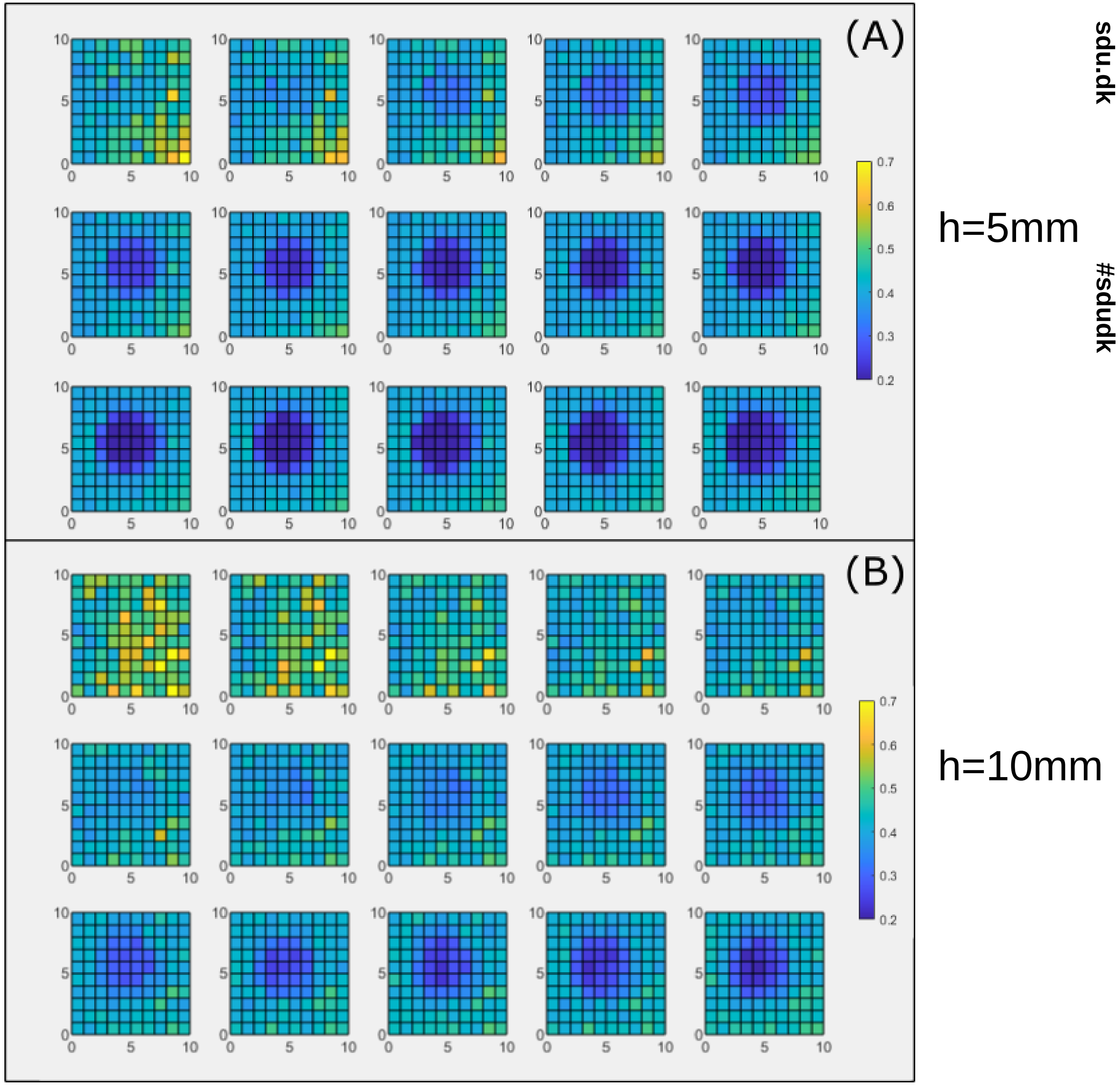

Cheng, Zhuoqi, and Thiusius Rajeeth Savarimuthu. "A novel robot-assisted electrical impedance scanning system for subsurface object detection." *Measurement Science and Technology*, 2021

Parameter estimation

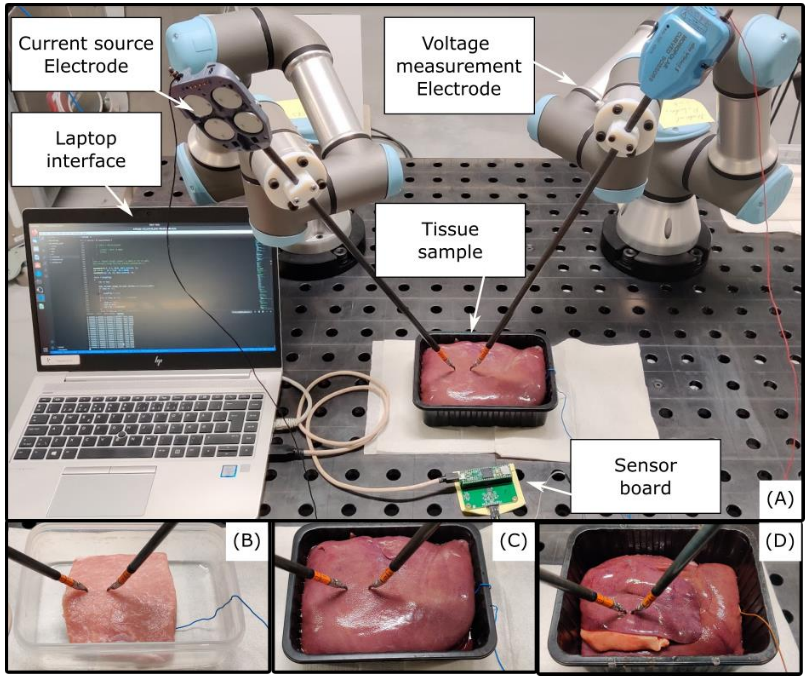

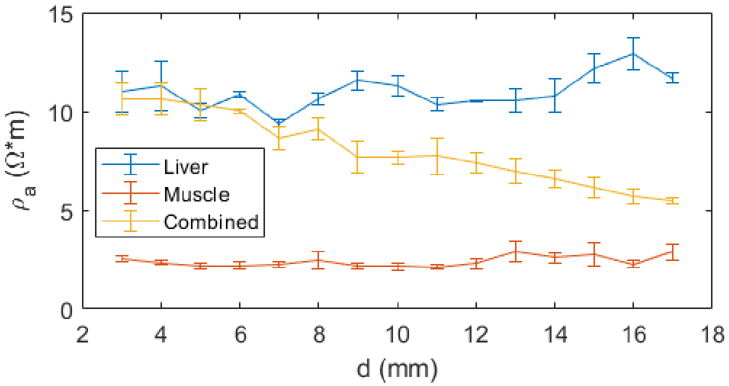

$$V_{MN}^{*} = \frac{I}{2\pi\sigma_1}\left(\frac{\Delta d}{d(d+\Delta d)} + 2\sum_{n=1}^{\infty}\left(\frac{\boxed{k}^n}{\sqrt{d^2+(2n\boxed{h})^2}} - \frac{\boxed{k}^n}{\sqrt{(d+\Delta d)^2+(2n\boxed{h})^2}}\right)\right)$$

$$\boxed{\rho_a(d) = \rho_1\left[1 + 2\frac{d(d+\Delta d)}{\Delta d}\sum_{n=1}^{\infty}\left(\frac{k^n}{\sqrt{d^2+(2nh)^2}} - \frac{k^n}{\sqrt{(d+\Delta d)^2+(2nh)^2}}\right)\right] = \underline{\rho_1(1+\alpha)}}$$

Algorithm 1 Pool of candidates generation

if $\rho_a(d_1) > \rho_a(d_0)$ **then**
  k^* = 1
else
  k^* = -1
end if
for $k = 0$ *to* k^* **do**
  for $\alpha = 0$ *to* $2k/(1-k)$ **do**
    $\rho_1 = \rho_a(d_0)/(1-\alpha)$
    for $h = 0$ *to* d_1 **do**
      for $d = d_0$ *to* d_1 **do**
        calculate $\tilde{\rho}_a(d)$ using Eq. (8)
      end for
    end for
  end for
end for

Search algorithm: Nearest Neighbour

Parameters estimation:
*ρ*1 = 10.99Ωm, *ρ*2 = 3.66Ωm, *h* = 6mm.
Fitting error Err=0.016 Ωm.

Cheng, et al. "An electrical bioimpedance scanning system for subsurface tissue detection in Robot Assisted Minimally Invasive Surgery." *IEEE Transactions on Biomedical Engineering*

Active search =

The post processing time is 0.13s.
For each vertex, it takes 8s for VME to scan.
In total, it takes 16 min to complete the scanning of a 11*11 grid mesh.

Use **Gaussian Process** to estimate the conductivity distribution;
Use **Bayesian Optimization** to determine the next sensing point.

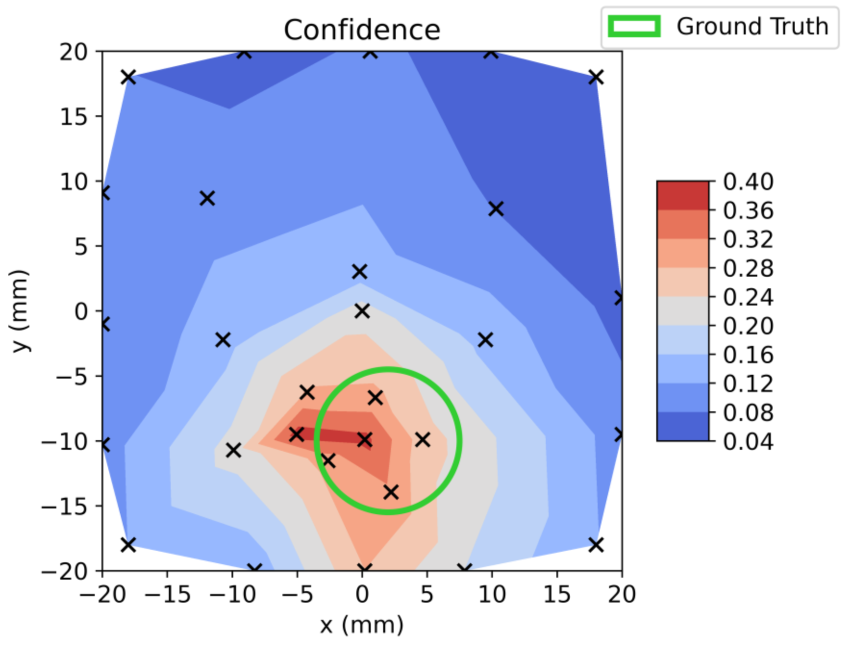

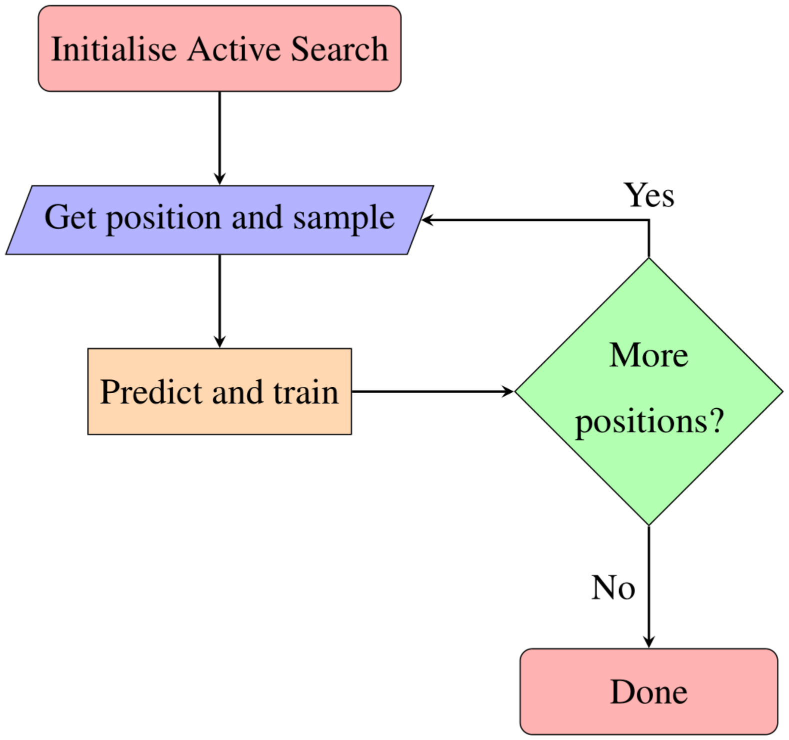

Cheng, et al. Active search of hidden lymph node using Robot Assisted Electrical Impedance Scanning. IEEE TIM

Gaussian process regression

Multivariate Gaussian distributions

$N(\mu, \Sigma)$

Gaussian processes

$GP(\mu(x), K(x, x_*))$

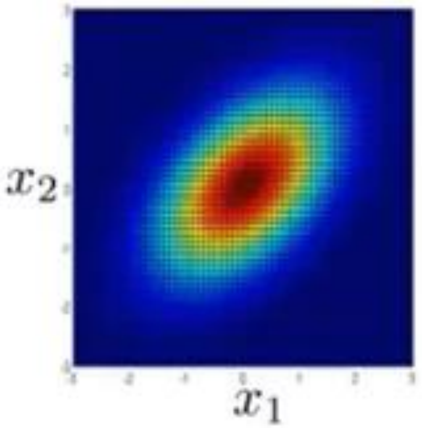

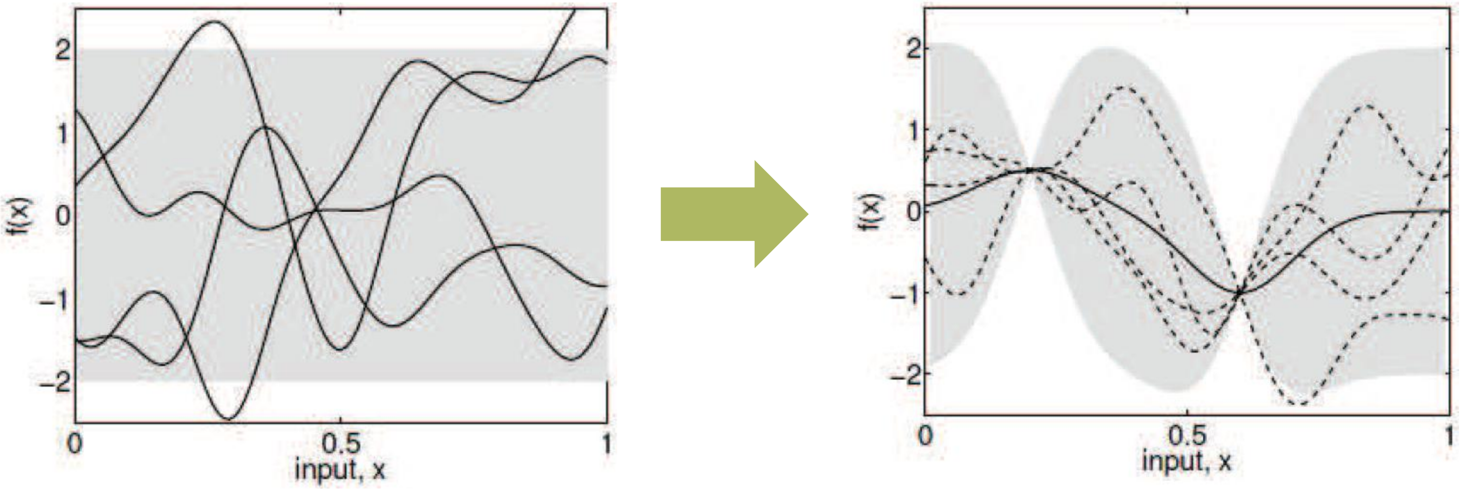

we observe a training set $\mathcal{D} = \{(\mathbf{x}_i, f_i), i = 1 : N\}$, where $f_i = f(\mathbf{x}_i)$

Given a test set $\mathbf{X}_*$ of size $N_* \times D$, we want to predict the function outputs $\mathbf{f}_*$.

A Gaussian Process is a Gaussian distribution over functions:

Assumption:

$$\begin{bmatrix} f \\ f_* \end{bmatrix} \sim N\left(\begin{pmatrix} \mu \\ \mu_* \end{pmatrix}, \begin{bmatrix} K & K_* \\ K_*^T & K_{**} \end{bmatrix}\right)$$

Mean function: μ(x)

Covariance function: $K(x, x')$

$$K(x, x') = \sigma_f^2 \exp\left(-\frac{1}{2\ell^2}(x - x')^2\right)$$

$K(x, x')$ is the kernel.

The prediction of sampling location x_* using GP regression:

$$p(f_* | X, f, X_*) \sim N(f_* | \mu(X_*), \sigma(X_*))$$

where

$$\mu(X_*) = K(X_*, X)\,[K(X, X) + \sigma_{noise}^2 I]^{-1} f$$

$$\sigma(X_*) = K(X_*, X_*) - K(X_*, X)\left[K(X, X) + \sigma_{noise}^2 I\right]^{-1} K(X, X_*)$$

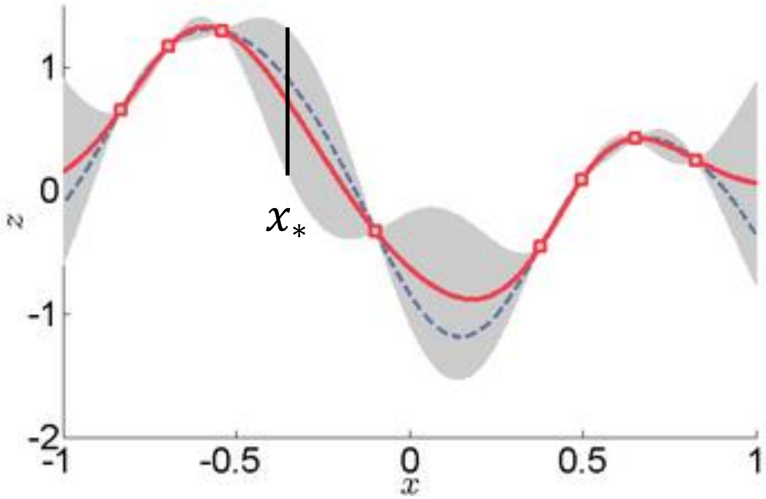

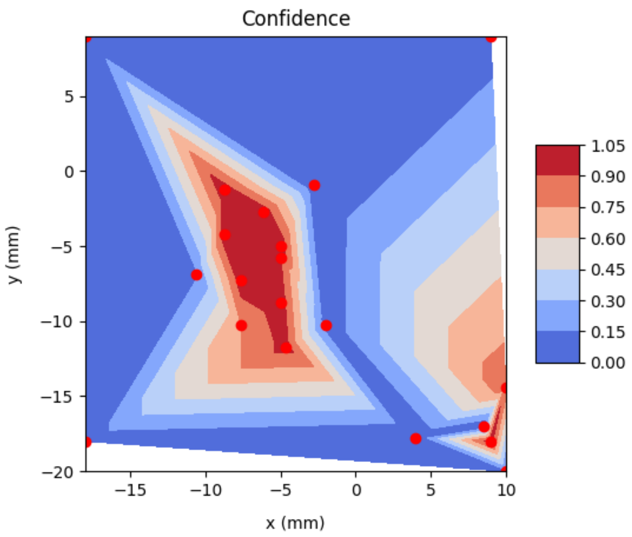

Subsurface object existence likelihood: f(x,y)

Bayesian Optimization

Query the next point by an **acquisition function:** trade-off between exploitation $\mu(x)$ and exploration $\sigma(x)$.

Acquisition function: **Expected Improvement**

$$EI(x) = \begin{cases} (\mu(x) - f(x^+) - \xi)\Phi(Z) + \sigma(x)\varphi(Z), & if\ \sigma(x) > 0 \\ 0, & if\ \sigma(x) = 0 \end{cases}$$

where

$$Z = \begin{cases} \dfrac{\mu(x) - f(x^+) - \xi}{\sigma(x)}, & if\ \sigma(x) > 0 \\ 0, & if\ \sigma(x) = 0 \end{cases}$$

- $\Phi(Z)$ and $\varphi(Z)$ are the cumulative density function and the probability density function respectively.
- ξ is a hyperparameter for tuning exploration and exploitation.

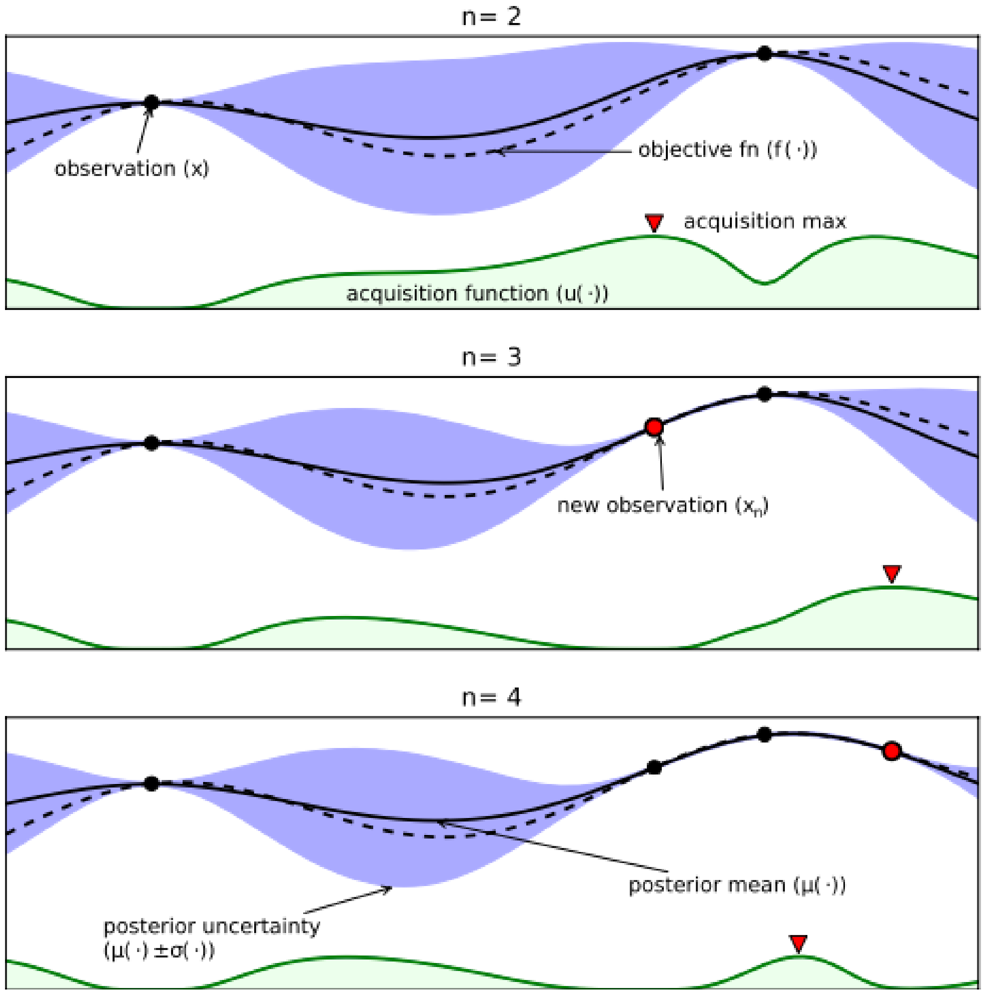

Active Search in Subsurface lymph node detection

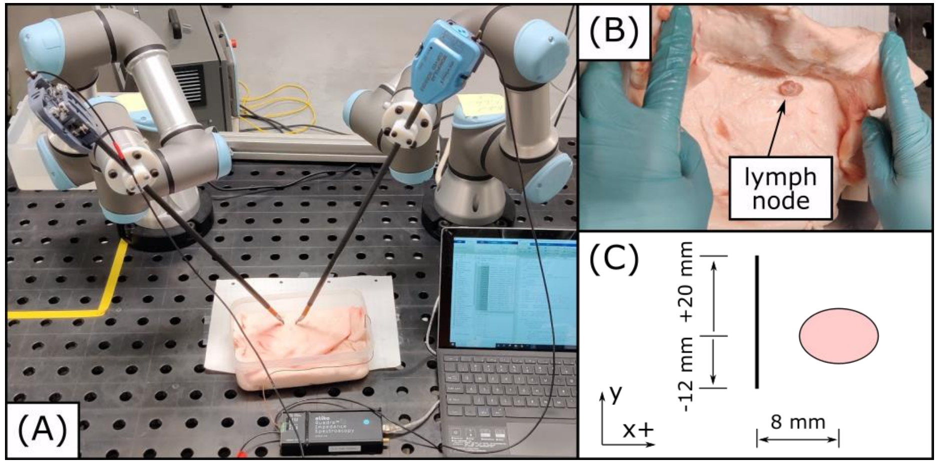

- Compared to the grid scanning, the Active Search method has higher precision, and recall;
- The AS method takes about 4min to explore the area and localize the lymph node.

Cheng, Zhuoqi, et al. "Active Search of Subsurface Lymph Nodes Using Robot-Assisted Electrical Impedance Scanning." IEEE Transactions on Instrumentation and Measurement, 2022

Sensing on curved tissue surface

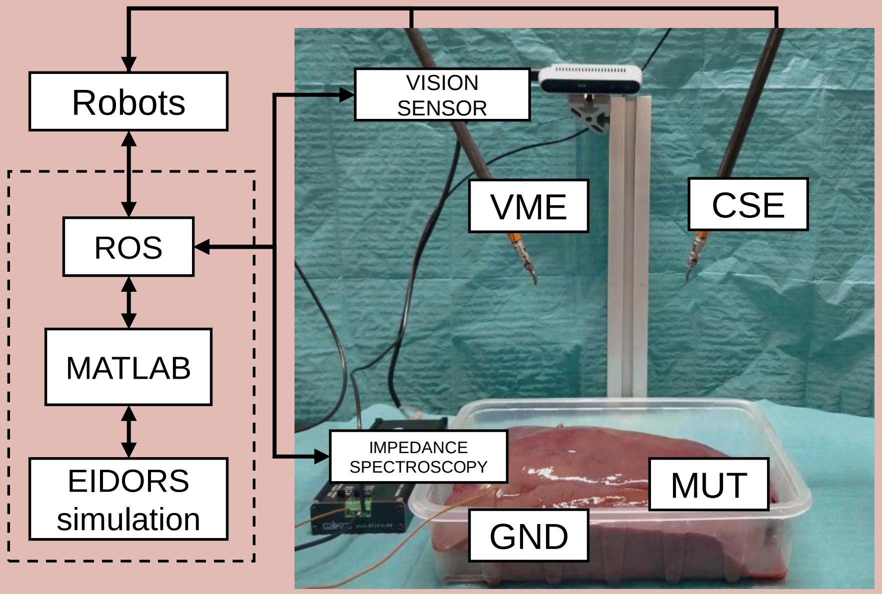

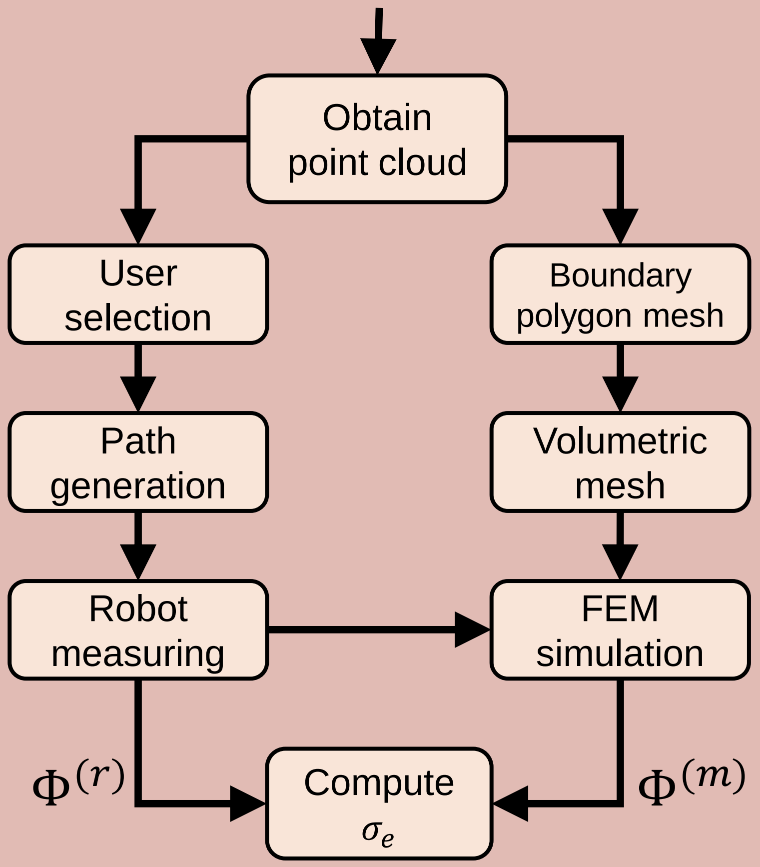

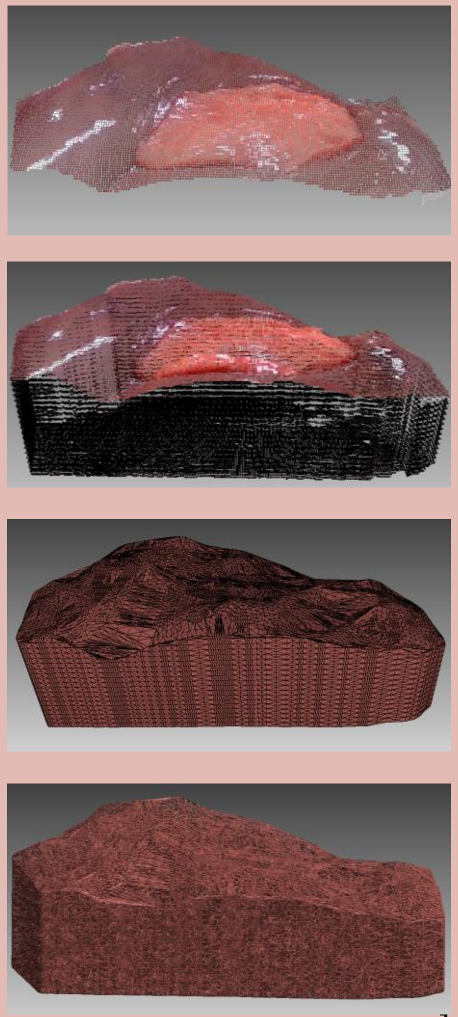

$$\frac{\sigma^{(r)}}{\sigma^{(m)}} = \frac{\Delta\Phi^{(r)}}{\Delta\Phi^{(m)}}$$

Piccinelli, Marco, et al. "3D Vision Based Robot Assisted Electrical Impedance Scanning for Soft Tissue Conductivity Sensing." *RA-Letter*

RAEIS sensing on curved tissue surface

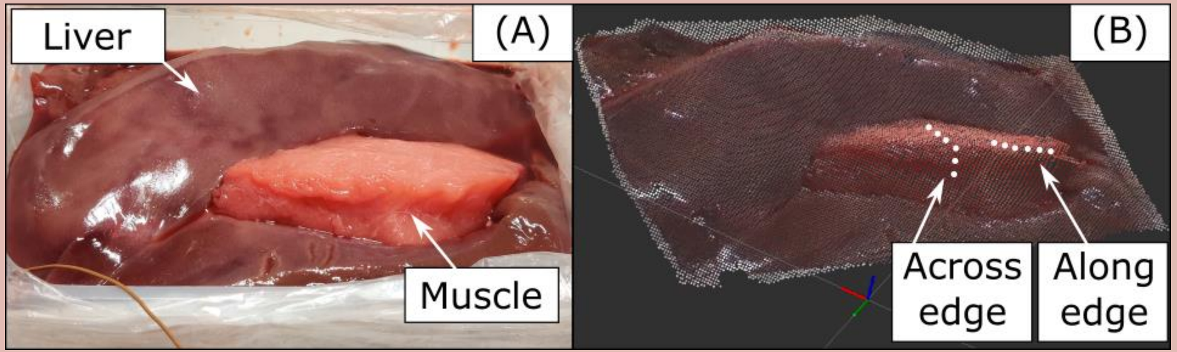

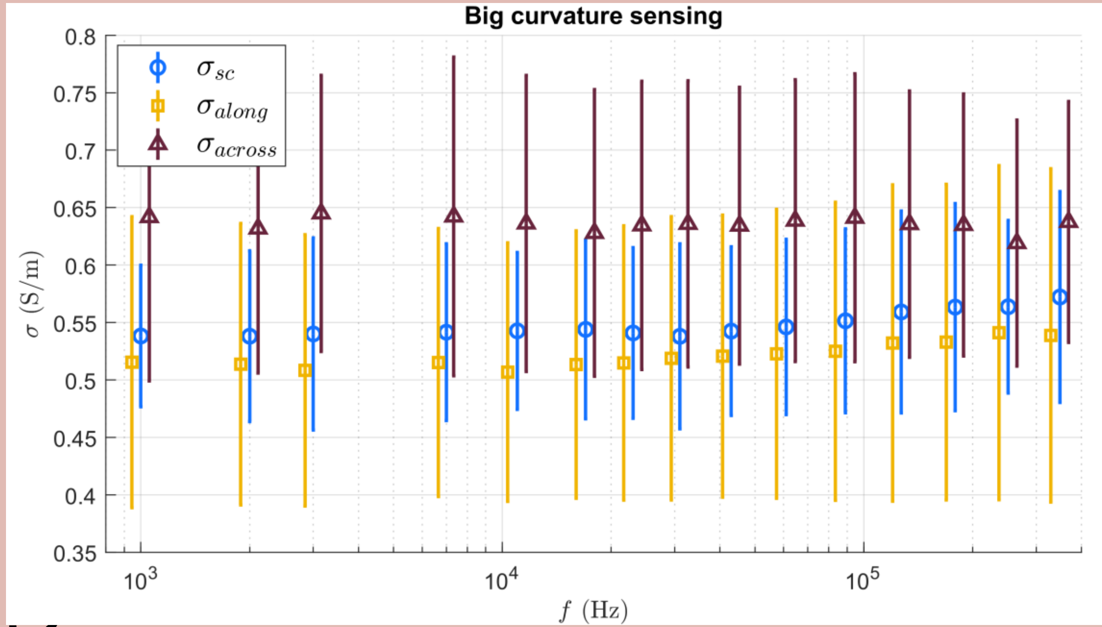

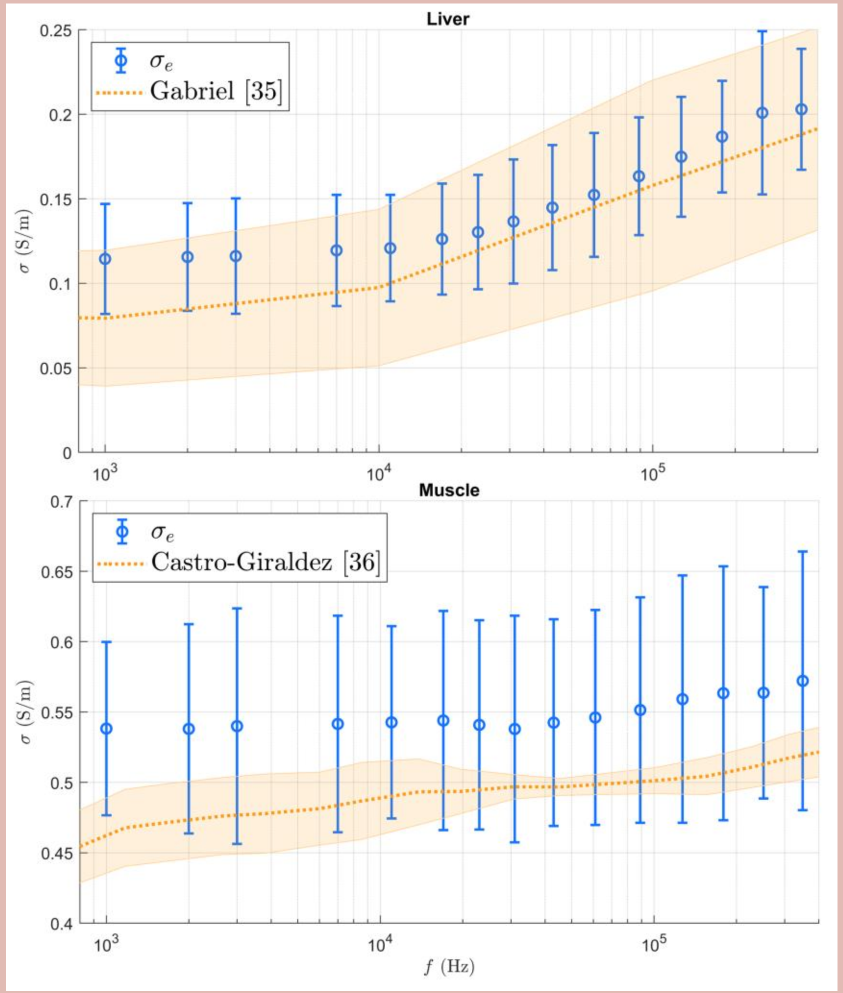

Piccinelli, Marco, et al. "3D Vision Based Robot Assisted Electrical Impedance Scanning for Soft Tissue Conductivity Sensing." RA-Letter

Summary

Robot Assisted Electrical Impedance

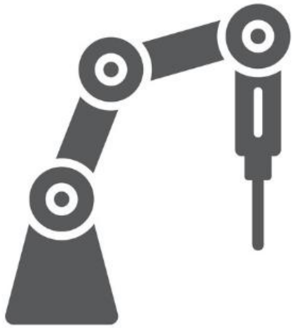

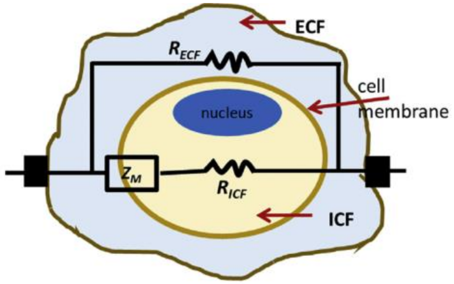

Medical Robotics

Electrical Bioimpedance

→ Robot can improve the EBI sensing flexibility, efficiency and stability;
→ EBI sensing can be an important sensing modality in robotic system for robotic surgery.

Crack detection/ material homogeneity

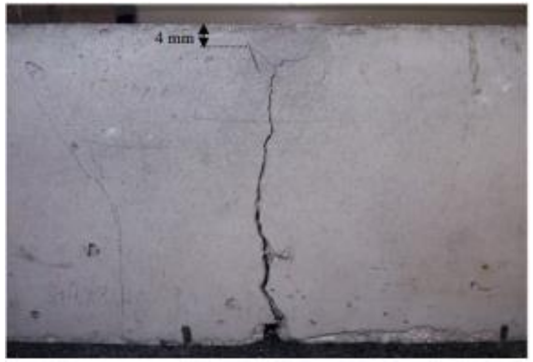

Biomimetic robot